Ice interaction processes during ice encroachment

Bridges, Robert; Riska, Kaj; Hopkins, Mark; Wei, Ying

DOI
10.1016/j.marstruc.2019.05.007

Publication date
2019

Document Version
Accepted author manuscript

Published in
Marine Structures

Citation (APA)
Bridges, R., Riska, K., Hopkins, M., & Wei, Y. (2019). Ice interaction processes during ice encroachment. *Marine Structures*, *67*, Article 102629. https://doi.org/10.1016/j.marstruc.2019.05.007

ICE INTERACTION PROCESSES DURING ICE ENCROACHMENT

Robert BRIDGES[1], Kaj RISKA[1,5], Mark HOPKINS[2], Ying WEI[3,4]

[1]Total S.A. E&P, [2]RealIce, [3]Stagiare at Total S.A., [4]Aalto University

[5]Presently at Delft University of Technology

Ice encroachment is the accumulation of ice atop a platform and results when ice drifts against a platform. Most often this occurs in shallow water but in principle can occur in deep water if the ice drift length is long enough. As the ice drifts against the platform it is broken and generates rubble and ice piles in front of the platform, and with sufficient drift duration blocks of ice can be pushed up and onto the platform. This must be taken into account when designing structures in the Caspian Sea and other shallow water areas where there is significant ice drift. Ice can encroach on the structure by ice ride-up and pile-up. Consequently, the height and extent of the ice piling up on top of the structures must be taken into account in designing the layout, and often a protective ice encroachment zone is made all around the structure. The aim of this paper is to provide an outline of various approaches and parameters to consider where ice encroachment may occur. The study is supported by analysis of dedicated ice model test data, numerical simulations using Discrete Element Models, and full scale data of ice encroachment events. The intent is to give an understanding of the physics of ice encroachment and support in the design of shallow water offshore structures. In particular, the results indicate the importance of ice strength in the process and especially the maximum pile height. If the ice is weaker, the pile grows horizontally in a seaward direction in front of the structure, and conversely, stronger ice forms ice encroachment with greater vertical and also horizontal extent on the platform. The results also show that once the maximum pile height is established subsequent drift enlarges the seaward extent of the rubble pile in front of the structure.

Keywords: Ice Encroachment, Rubble Ice, Offshore Structures, Pile-up, Ride-up, Discrete Element Modelling.

1. INTRODUCTION

Ice Encroachment (hereinafter referred to as IE) is a general term describing ice that advances on to a platform or structure, as shown in Figure 1-1. Ice encroachment takes place when the oncoming ice sheet impacts against a structure, and ice is first crushed followed by a bending failure which is sometimes caused by buckling. The broken ice floes form a rubble pile in front of the structure. This rubble pile creates a slope along which the ice can be pushed up and onto the structure. The processes involved in IE are analysed in this paper, from the beginning process of rubble pile creation to the point at which the ice ends up on the platform.

The IE process requires a large body of water as significant ice encroachment is created only if a large expanse of ice is allowed to drift. The expanse must be sufficiently large to allow for enough wind ‘fetch’ to drive the process. The driving force comes from the wind blowing over many kilometres of ice. The wind couples to the ice through the boundary layer which is influenced by the ice surface roughness. The expanse of ice need not be uniform, but a degree of continuity is required so that forces are able to transmit over a large distance. Once the ice sheet is moving, the wind continues to push the ice sheet against the structure, or shore. An example of shore rubble pile is shown in Figure 1-2. This pile eventually induces ice encroachment by providing a path for the ice to ride up onto the structure. With sufficient driving force and slope the ice sheet can continue to push in a horizontal direction along the structure top. This is termed a ride-up event. In contrast, a pile-up is considered when the rubbling process is predominantly in a vertical direction.

Figure 1-1. Example of Ice Encroachment ride-up event in Caspian Sea. Source: Mckenna et al. (2011).

Figure 1-2. Shore ice rubble and pile-up in Sabetta. Source: Coche and Kalinn (2013), credit AARI.

1.1 Review of Existing Knowledge on IE Process

Very little published data exists with respect to ice encroachment, and so analogies to similar situations must be made, such as rubble ice formations, shore inundation and ice pile-ups on structures. The following discusses some of these, however it is acknowledged that this is not exhaustive, and is intended to simply provide some insight into the processes that are related to IE.

Ice encroachment in the Caspian Sea is specifically reported by Mckenna et al. (2011). In this paper the distinction is made between ride-up and pile-up events. It also reports on observed IE events and gives a maximum height formulation, as well as discusses attributes such as the apex position, slope angles and effect of freeboard. In particular, the authors note that the steepness of the front slope may increase the forces on the ice sheet at the foot of the pile, and in this case the pile forms further back from the structure. The paper, however, provides limited discussion on the processes and modelling. For these we have to look at other work not directly related to IE; studies on pile-up and ride-up, such as Kovacs (1982 & 1983) which cover coastal pile ups in the Bering Sea and on the coasts of Alaska, provide a useful reference. The piles were observed to form by compressive forces acting along the fast ice edge, and with low driving forces (100 kN/m). Ride-up events were noted to extend 50 m onto the shore. The composition of the rubble included ridges and rafted ice, with a range of ice thickness from 0.3 to 2.0 m. Fragments with soil were also observed suggesting ice was pushed down to the seabed and then brought back up. Earlier work by Taylor (1978) also provides details of shore ice piles and grounded ice ridges that are reported up to 30 m high along the northern coast of Somerset Island. The ice ridges were composed of 1 to 2 m thick ice blocks. Ice features were observed 185 m inland across the beach when an 8 km long ice floe struck the shore resulting in 11 m high ridges. As with Kovacs, winds did not exceed 15 m/s, which suggests that strong winds are not required for the formation. Lepparanta (2013) also reported examples of ride-up and shore pile-up in the Baltic.

One of the most insightful works on the understanding of the IE process is by Christensen (1994), which considers the ice interactions during rubble pile-up and ride-up on sloped structures and events along the coast of Denmark. Methods for deterministic design are provided for 2D (vertical plane in direction of ice drift) in plane forces. In particular, piece size influence and how this affects stability is discussed and related to the limiting horizontal failure pressure of the ice sheet. Further, ride-up criterion is related to the frictional resistance and also to the kinetic energy. Pile-up events are related to ice strength (due to deformations causing instabilities) rather than the driving force of ice. The pile-up height is then discussed based on two methods; Kovacs and Sodhi (1980), where height is related to driving force overcoming gravity and friction, and Allen (1970) where height is related to lifting the rubble pile. Further, three limit mechanisms are noted; limited driving forces, ice strength and kinetic energy.

There have also been studies using ice model tests, such as Sodhi et al. (1983), which present results for a shore (sloped) structure with obstructions (sea defense elements) and roughness elements. Another informative article is Yoshimura & Inoue's (1985) investigation of rubble ice around a gravel island. The test was made in two stages; with thick ice, and then thicker ice with rubble. Of note is that the tests required 6 mm thickness (strength 14 MPa) to create realistic failure process. The height of the piles were compared to Croasdale (1978), with lower calculation results attributed to model ice not being as brittle as actual sea ice and support accounted for only using buoyancy forces and neglecting any support from the ice pile. A further series of observations from ice model tests are presented by Repetto-Llamazares et al. (2013), which provides insight into the ice rubbling process for a shoulder ice barrier and the influence of the inclination angle of the sloped structure on the stability of broken ice pieces. Another noteworthy set of ice model tests were performed for Northstar Island rock berm protection schemes as presented by Li et al. (2009). The significance of the ice properties, ice thickness, elastic modulus and structure geometry at or near waterline are noted to have an influence on the process. Thicker ice tended to produce ice ride-up, while thinner ice results in rubble and favours pile-up. In addition, the elasticity of ice appeared to have an influence whereby lower elastic moduli tended to promote ice ride-up.

Studies on shore pile-ups provide useful insights into the process, however much can be gained from studies of events of grounded ice rubble. For example, Timco et al (1989) investigated the horizontal and vertical load apportioned through the rubble to the berm and that of the structure using ice model tests. Of interest is the sequence of pile-up during the test progression, shown a with schematic of the geometry of rubble as function of time (seconds). The tests also included a range of ice strengths, however no clear trend was observed in the load apportion, but some change was observed with a rougher berm. Results indicate that 50 to 70% of the ice force is transferred to structure. This was also observed in Timco (1991) where large scale buckling events were observed as a frequent failure mode, as well as upward/downward bending and localised crushing. In the case of ride-up event (inclined slope), ice accumulated on top of rubble until a critical level was reached and large scale bending failure occurred and rubble would then slide down. The full scale observation paper by Timco & Wright (1999) notes the load attenuation at Tarsuit Island with rubble pile formation. Sayed (1989) also provides examples of load transmission though grounded rubble ice where the main focus is made on Beaufort Sea rubble settlements, as outlined by observations by Kry (1977). Evers and Weihrauch (2004) also investigated ice loads and rubble formation by ice model tests, and also of ice barriers. Vertical and inclined piles were used with variation in spacing, which affected rubble generation. Ice model tests by Karulin et al (2007) showed a load increase in the initial stage of underwater pile formation, and a reduction observed when stationary grounded pile-up formed, where the change in load is considered related to seabed friction.

Reports on observations of grounded rubble formation are equally valuable to understand the processes involved, such as Allyn and Wasilewski (1979) on artificial islands in the Canadian Beaufort Sea (30 m water depth). In particular, they noted the influence of freezing of void spaces (on rubble shear strength). Other ice rubble formation observations include Neth (1991) along the Molikpaq in water depths of 20, 14.5 and 11.5 m. The instability during the initial floating pile is noted and the conditions required for rubble formation, such as:

- Ice drift perpendicular to structure (caisson face)
- 10/10 concentration
- Shallow water depth
- Long structure (caisson face)
- Low drift speed

Observations note that the slope angle initiated flexural failure and the ice fell back onto the ice sheet, generating broken ice blocks and formation of floating rubble. Failure processes observed include crushing, flexure, and buckling (as well as mixed mode).

Observations by Crocker et al. (2011) of Caspian Sea stamukhi and pressure ridges provide information on the dimensions of seabed disturbances (pits) that form underneath stamukhi (for the design of offshore pipelines). The stamukhi observed during the programme were made up of ice blocks typically 0.10 m to 0.20 m in thickness. Interestingly, the stamukhi-building process is considered to involve 4 main modes, described as ‘ramp-up’, ‘turn-over’, ‘rubbling’, and ‘keel-building’. In particular in the ‘rubbling’ mode, flexural or buckling failure is reported to occur usually near the base of the slope. Both upward breaking and buckling of the ice have been observed, and some crushing as well. Keel building is noted as being from downward breaking in flexure and ramp down (with the latter creating greater seabed forces).

Many other references exist on this topic, such as Barker and Timco (2016) which analyses the rubble fields from Beaufort Sea operations, and Barker & Timco (2007) presents rubble events during series of storms for Isserk I-15. A useful compilation is provided by Barker & Timco (2017). This provides a summary of ice rubble events from the Arctic (mainly Beaufort), Temperate regions (Baltic, Caspian & Canadian), and offshore Sakhalin. The maximum pile heights are collated and analysed using various empirical relationships, alongside the full scale event data. Interestingly, the simulation results and full scale data indicate water depth to have limited relationship with rubble heights although with much scatter.

Various simulations of pile-ups have also been performed and whilst they all cannot be mentioned here, a selected few are included to provide examples. 3D modelling of shore pile-up has been carried out, for example by Barker et al. (2001). Whilst earlier work by Marshall, Jordaan & McKenna (1991) proposed a 2D model of grounded ice rubble using spring and dashpot model. Finite element modelling of rubble ice was used by Gürtner et al. (2008). Goldstein et al. (2013) presents a 2D DEM simulation of grounded ice pile-up on slope structure. These simulations all use different methods. The ice piece instability with loss of block connection at top, middle way or at sheet edge to rubble is mentioned in Croasdale (2012) which discusses the rubble loads based on a limit force approach from the pack ice pressure in the ridge building process. Ice rubble interactions are categorised into three cases; ice sheet failing in flexure and ramping over ice, ice sheet failing in flexure and turned underwater, and footing failure mode. Here, the flexure failure mode calculations are based on earlier work (Croasdale 1994) and the latter based on soil mechanics. Of note, is the comment that the strength of rubble is dependent on aging process and internal stress. Sail height values are presented using ice thickness, $h^{0.5}$, based on ridge correlation (Tucker and Govoni 1981). The results are presented predominantly with ice thickness dependency. The rubble height is also considered by McKenna et al. (2008) based on empirical formulation (unfortunately not given) with distribution and extent based on a parabolic function. Input values for the calculation requires the length of ice (drift speed x event duration), thickness and porosity. Of note is that the rubble height calculation is determined from a function of two distributions; using mean level ice thickness and then using mean rubble ice height.

A final mention should also be made for rubble piles in instances without grounding, such as Mayne and Brown (2000) and later ElSeify & Brown (2006), which reports on the ice piles from Confederation Bridge Monitoring Programme. Observations note that the rubble pile formed from upward bending or crushing, whilst floe splitting and plug failure lead to ice collapse/submerge and clearing. The influence of snow increasing friction is also noted, leading to steeper ice pile (of 45 degrees). The maximum pile height is also considered, for example by Maattanen and Hoikkannen (1990). Interestingly results for increase in ice thickness and velocity are presented and indicate reduced pile height; contrary to results for grounded rubble piles. The ice strength has also been investigated by Izumiyama et al. (1994), noting here four types of rubble types in front of a conical structure and failure modes related to ice thickness and (flexural) strength. They also looked at correlation of loads with piece size. Many models have also been developed on sloped structures to investigate rubble loads, such as 2D FE-DE model by Paavilainen (2013) used in comparison with results of model tests by Timco (1991) and Saarinen (2000), and resulting peak loads were reported as being related to vertical pile movement and a load drop linked to buckling of force chains. The importance of buckling as a failure mode is also highlighted in recent work by Ranta et al. (2018).

1.2 Purpose of Study

It is clear from the existing studies that IE is a complex process and whilst much is reported on related phenomena, very little is in the literature on the processes and parameters specific to ice encroachment. This study is intended to address this deficiency. An outline of the parameters influencing the process is supported by analysis of dedicated ice model test data and Discrete Element Model (DEM) as well as observations from full scale ice encroachment events. The study provides examples of calculations and analysis of data that try to clarify the effect of using different ice parameters, as well as some recommendations and considerations for the design of structures exposed to ice encroachment.

The paper is divided into six sections. The first section provides a summary of the ice encroachment process. The next covers the modelling approach, using DEM, verification from ice model tests and full scale data. We then investigate the different ice parameters influencing ice encroachment. Based on the analysis, observations of the IE process are presented, and then how these can be influenced by design arrangements. Finally, a short summary of the findings is presented.

2. OVERVIEW OF THE IE PROCESS

It is clear the IE includes several different physical processes related to ice failure and deformation, such as crushing, buckling and bending, sliding, submergence and force chain formation. Several structural and ice parameters should therefore be included when considering the ice encroachment process:

- Effect of structure freeboard and water depth
- Structure width and cross section profile (sloped/vertical)
- Ice event duration and drift angle with respect to the structure face
- Ice protection structures
- Effect of friction on seabed and structure
- Effect of snow on ice-ice friction
- Effect of time – consolidation of keel and rubble, and continuity of driving force
- Through thickness ice parameters
- Hydrodynamic effects
- Porosity of the ice pile
- Initiation conditions – slopes, build up rates
- Ice drift speed, angle and edge shape
- Ice properties (thickness, strength and stiffness)
- Bridging of ice between structures or rubble piles.

This list is not exhaustive but indicates the range and variation of parameters influencing the process. In this study we consider some of the contributing parameters to IE.

2.1 Stages of IE

The physical processes of creating and controlling an ice pile-up and especially ice encroachment involve several different types of forces. The relative magnitude of these forces is dependent on the structure arrangement, ice properties and environmental conditions (water depth, etc.). The dominating process varies depending on the stage of process.

If we consider the process leading to ice encroachment on vertical structures, this proceeds in some distinct stages. Initially the ice fails by buckling or, in early phases of interaction, by crushing against the face of the structure. As the oncoming ice sheet breaks repeatedly against the structure, a rubble pile accumulates in front of the structure.

The ice rubble accumulation gradually fills the area in front of the structure to create a slope. In shallow water the bottom of the rubble accumulation will reach the seabed quickly. This is called grounding. Grounding stabilises the ice accumulation. Additional incoming ice increases the height and extent of the pile. See Figure 2-1.

The next stage of the encroachment process begins when the top of the pile reaches the level of the structure. Once the pile height reaches the level of the structure, the ice sheet is able to push ice blocks onto the top of the structure. The ice accumulation atop the structure is called ice encroachment. In the subsequent discussion we use pile-up to refer the vertical enlargement of the rubble pile and ride-up to refer to the ice sheet riding up and over the pile. Note that the ice action on an inclined structure reverts to the pile-up process if the structure angle is close to vertical (more than, say 70^{o}), see also Figure 2-2.

When the ice pile is grounded, ride-up process may dominate, depending on ice strength as discussed later, pushing ice up the rubble pile and onto the shore or structure. The limit for the pushing length is set by buckling strength of the chain of ice floes. . Ultimately, the growth of the pile is limited by the strength of the ice sheet that is pushing the ice up the pile. As the pile grows the force required to push ice blocks to the top of the pile grows as well. This force is provided by the oncoming ice sheet and must be transmitted through the sheet. Eventually the force will reach a level that exceeds the buckling strength of the sheet. At this point the encroachment will cease and the buckling failure creates more blocks that add to the ice pile. As long as the wind continues to push the sheet, the sheet will continue to fail against the pile and enlarge the rubble pile horizontally ahead of the structure.

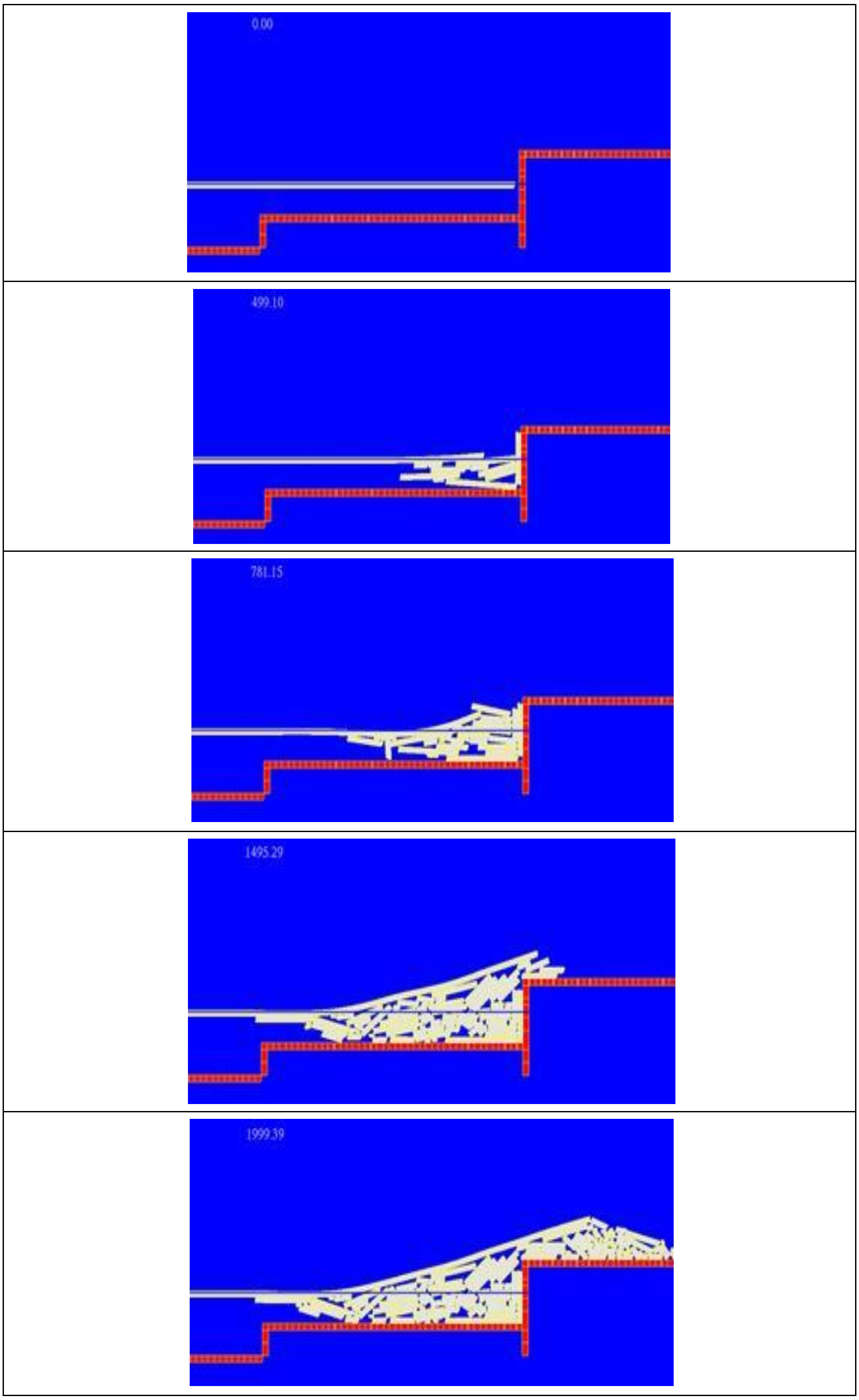

Figure 2-1. Stages of ice interaction and encroachment illustrated with 2D DEM simulation. Solid structure is shown as red and the ice sheet is moving towards the right. The process begins with initial contact and breaking with the formation of a rubble pile. This pile then grounds and provides a slope for the oncoming ice sheet to slide over and onto the structure resulting in ice encroachment.

2.2 Ride-up and Pile-up

When an ice sheet is pushed against a structure with vertical face, ice is first crushed followed by failure induced by buckling of the ice sheet leading to failure in bending. The crushing – bending cycle is repeated many times to form a rubble ice pile in front of the structure. The rubble pile forms an upward sloping path to the top of the structure. This is especially likely to occur in shallow water where the pile becomes grounded. Ride-up against a vertical structure occurs when sufficient ice is piled up against the face of the structure to allow the advancing ice sheet to climb the sloping pile and reach the top of the structure.

Ride-up refers to ice floes lining up to form a force chain which pushes ice up the slope formed by the rubble pile in front of the structure or on the inclined wall of the structure, as seen in the last two stages in Figure 2-1. Ride-up requires a chain of floes that push each other up the slope. Ride-up distances can be considerable and interrupted only if the chain of floes or ice sheet buckles. Ride-up also depends on the inclination angle of the structure, on smaller inclination angles no ice pile-up is required to cause ride-up, see Event A in Figure 2-2 for sloped structure.

Simplified schemes of ride-up and pile-up are illustrated in Figure 2-2, where ice parameter dimensions include the rubble height, H_{max}, ice encroachment length, E_w, and rubble angle θ, whilst structural dimensions are freeboard, h_{fb}, and water depth, d_s.

It should be noted that in Event A, encroachment can extend onto the structure a significant distance, until an opposing lateral force (to the ice drift) is created, e.g. by ice barrier, wall or friction, or other instability in the ice sheet is created. This situation is evident in the large shore encroachment events, with records of ice extent hundreds of metres onshore.

Event B in Figure 2-2 illustrates the pile-up formation. Here we suppose that there is an obstruction on the top surface of the structure such that encroachment changes from the lateral motion to one of vertical piling. For the vertical structure, this may be created from the change of corner angle at the edge of the structure, thus contact with the ice pieces in ride-up over the rubble ice is broken, i.e. a break in the force chains. In a slope structure this angle change is less acute and therefore probability for lateral motion rather than vertical pile-up is higher. Noteworthy here also is that a steeper slope angle results in an increase ‘reverse tipping’ of ice pieces, whereby the highest pushed ice pieces fall back onto the oncoming ice sheet.

Event	Structure	Illustration
Vertical structure	Event A. Ride-up when ice rubble reaches freeboard height	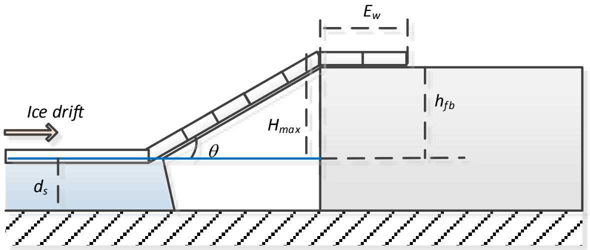
	Event B. Pile-up on structure (and ride-up over rubble)	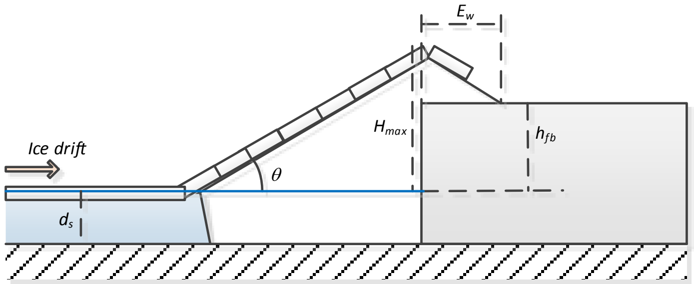
Slope structure *(inclination angle change in shade)*	Event A. Ride-up when ice rubble reaches freeboard height	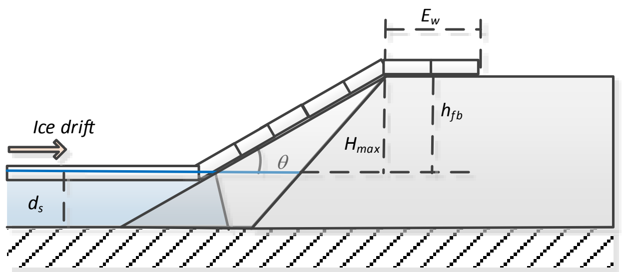
	Event B. Pile-up on structure (and ride-up over rubble)	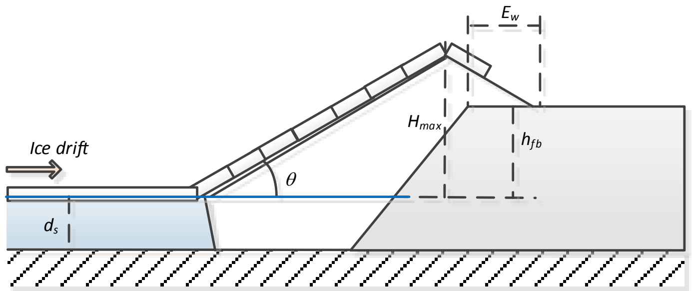

Figure 2-2. Illustration of ride-up and pile-up events for vertical and sloped structures.

2.3 Ice Actions during IE

When level ice drifts against a vertical sided structure, ice is first crushed which is followed gradually by repeated buckling - crushing cycle creating ice rubble build-up. The largest ice failure forces are generally considered to be caused by ice crushing. If the structure has inclined sides, the initial ice failure is in bending which after several ice crushing-beinding cycles is followed by rubble build-up. The force due to bending is smaller than that of rubble build-up, thus the largest forces are caused by rubble formation in the vertical case. These phases of horizontal force acting on the structure are well described in Palmer and Croasdale (2012). IE may be considered to have some specific considerations. In particular the ice actions resulting from the rubble process should be considered for the following two scenarios as identified by Sayed (1989):

1. *"Grounded rubble can transfer part of floating ice forces to the berm and thus reduce the loads on the structure.*
2. *Because a rubble fields width is larger than that of the structure, floating ice forces would act against a larger area and thus exert a larger total force on the rubble field. Therefore, a [floating] frozen rubble field would increase the forces on the structure that it surrounds."*

2.4 Description of the Ice Encroachment Geometry

The geometry of an ice encroachment pile cross section are shown in Figure 2-3. For design, the main parameter is the Ice Encroachment Length, l_{ie}. This depends on the ice encroachment height and the slope angles of the pile. Often all three of the slope angles (α_{fs}, α_{es} and α_{bs}) of the pile above water are assumed to be the same, around 20 to 30 degrees. Further, the ice encroachment height is considered independent of the structure freeboard based on the assumption of the asymptotic height; as when reaching this height the growth of the pile cross sectional area shifts to the front of the structure. The asymptotic height assumption is investigated later in the paper. The apex of the pile is generally considered to be close to the structure edge.

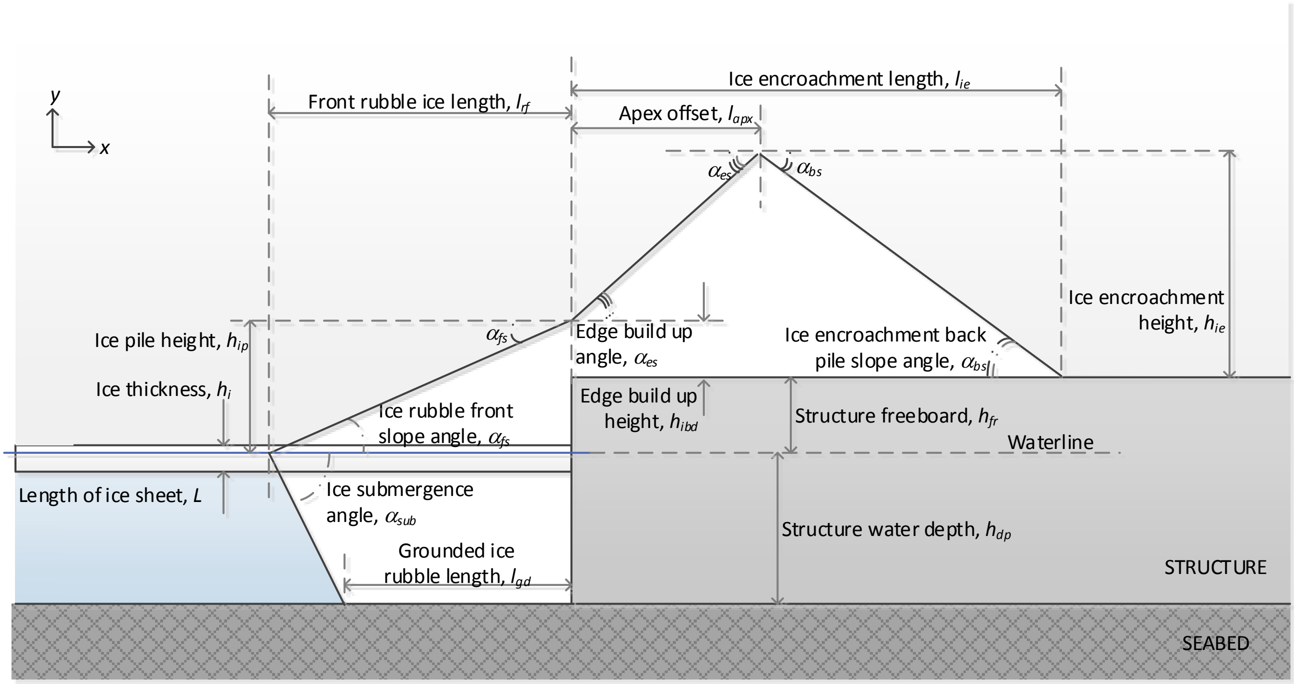

Figure 2-3. Schematic of geometric variables for IE (not to scale).

3. MODELLING AND VERIFICATION OF IE

The modelling of the IE processes and its verification may be performed by different approaches. Whilst use of full scale data is usually preferred, often all the exact information is not available and consists of the final pile dimensions rather than observations of the process. Thus, alternatively numerical and physical modelling approaches are often employed.

Physical modelling of ice encroachment is carried out in a model ice tank under controlled conditions. Because the ice tank is much smaller than an actual structure in an ice covered sea the ice tank model must be scaled down considerably. Scaling creates an acute problem for model tests because, while the modulus of ice, bending strength and compressive strength may be modified, it is impossible to independently scale all three properties at the same time. The interplay between these variables shape the ice encroachment process. For example, a stiff sheet with low bending strength or low compressive strength will tend to bore straight into the rubble pile and fail within the pile and have relatively low potential for encroachment. Conversely, a more flexible sheet with high bending strength will tend to override the rubble pile and have relatively high potential for encroachment. As it is hard to create an ice sheet with the correct balance between stiffness, bending and crushing failure modes it is not clear how accurately ice model tests can represent the ice encroachment process. In contrast, numerical models may be run at any scale. Unfortunately, numerical methods also have their own shortcomings.

The numerical methods that can be used to model such a problem are broadly speaking continuum finite element based and discontinuous discrete element (DEM) based. Finite element based methods use empirical constitutive models to describe, in an average sense, the ice fracture and rubble pile-up processes. These constitutive models use quantities like dynamic friction angles and passive pressure coefficients to quantify the ice strength. Discrete element methods model the motion and fracture of the oncoming ice sheet and the motion of the individual ice blocks broken from the sheet. Measurable ice properties such as thickness, modulus, tensile and compressive strength, and friction coefficient are used directly by the model. The level of abstraction in the discrete element approach is at a more basic level, namely, at the level of the failure process between elements, and the elastic-plastic nature of the contacts between loose blocks. Since the goal of this study is to provide insight regarding the probability of overriding ice pile-up at a structure expressed in terms of measurable ice properties we selected a discrete element method.

Unlike the physical model, in a numerical model it is possible, at least in principle, to tune the ice sheet stiffness and crushing and bending failure modes independently. However, this depends on how realistic are the constitutive models on which the failure modes are based. In this work we use a viscous-elastic approach to model the bending of the sheet and blocks, and a flexural failure model that includes finite crack energy. Modelling crushing failure with a discrete element model is inherently difficult because at the scale of the blocks the crystalline nature of the blocks and their failure is a sub-scale process. In theory, it may be possible to model compressive failure by finely discretising the blocks themselves, giving them a quasi-crystalline structure that allows the blocks to crumble under pressure. However, this entails a large computational penalty due to the huge number of fine-scale grains and a time step that must be reduced to compensate for the reduced grain mass. In the numerical modelling discussed below, ice crushing is not included. We assume that, while crushing dominates the earliest stages of ice rubble formation, once a small rubble pile has formed the sheet/rubble interaction causes flexural failure to dominate.

3.1 Ice Model Test Investigations

An extensive series of ice model tests has been carried out related to this study and the results in terms of parametric variation effect on ice encroachment are discussed in this chapter. The process of ice encroachment and pile-up height was investigated in these tests, for example as described by Bridges et al. (2016). The aim of the tests was to gain an improved understanding of the mechanical process of ice encroachment and knowledge on performing ice encroachment simulations and tests.

3.1.1 Observations during ice model tests

An overview of the ice encroachment process from the ice model tests is shown in Figure 3-1. The initial ice failure process was similar in all tests; first the ice was crushed against the structure and crushed ice piled up on top of the incoming ice (and down under the incoming ice). Initial crushing was followed by a change into repeated bending. This was followed by the onset of the pile-up process. The pile in front of the structure grounded and grew to the height of the structure freeboard. From this point there were differences in the ride-up process that depended on ice strength.

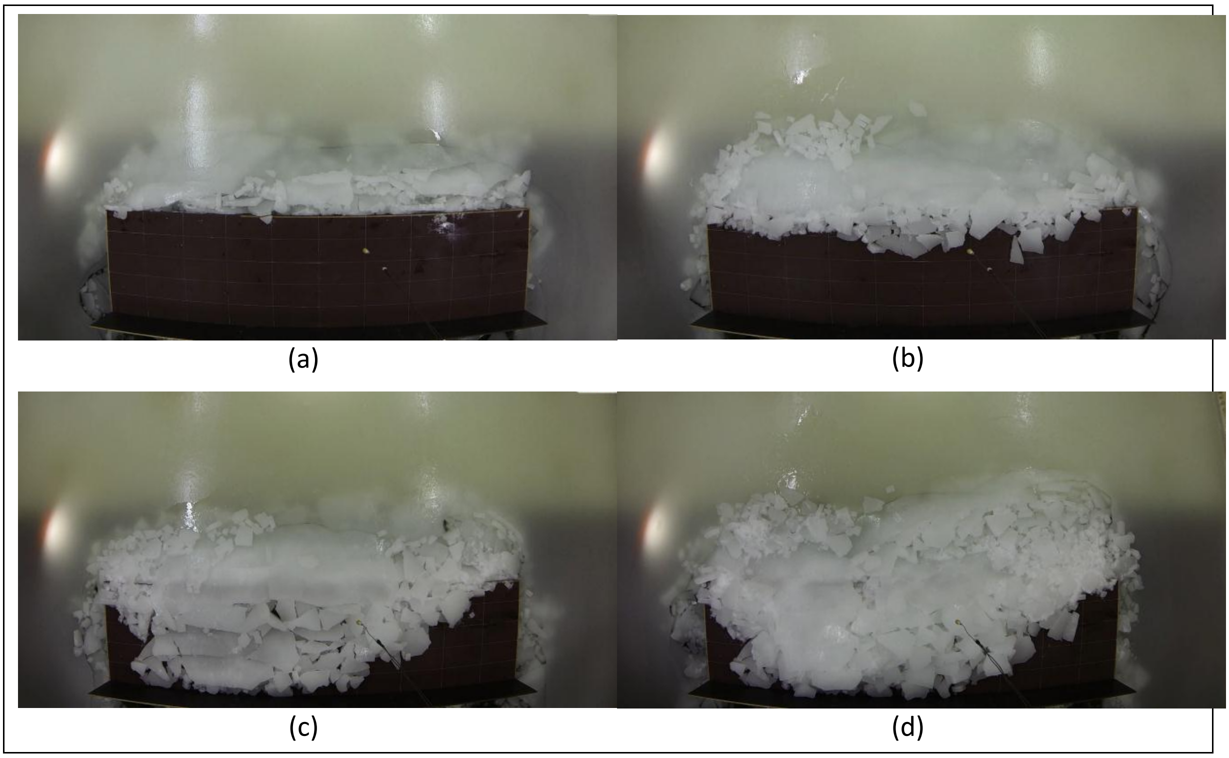

Figure 3-1. The pile-up and ice encroachment extent from top view taken from video snapshots during the ice model tests. Ice movement is downwards.

It should be noted that there were several modifications to the test program and parameters based on observations. In particular using a scale factor that provided a realistic ice strength (considered being a combination of bending, compressive strength and Young's Modulus) is important. The length related quantities, such as ice thickness, are scaled with the geometric scale factor λ. Strength and stiffness are also linearly proportional to the geometric scale. As the stiffness and strength parameters of model ice could not be scaled independently, the correct scale used in the tests is somewhat ambiguous. For example the original scale (λ = 25) was changed (to λ = 15), here it is important that the ice parameter values are known and then used, such as in the numerical modelling performed after the tests. The effect of the change in parameters was observed in testing with thicker ice which also was stronger in compression, as greater ice encroachment occurred. The water depth influenced the pile-up process so that the pile-up grew faster in more shallow water; this is natural as less ice is needed for pile-up in more shallow water. The ice encroachment length and height varied along the structure and systematic recording of the pile size was necessary. A snapshot from test is shown in Figure 3-2. Qualitative comparison between ice model test results and full-scale observations showed that the block sizes were generally comparable and the geometry of the ice rubble piles similar. Overall the observations during the testing and also the understanding of processes increased during the testing.

Figure 3-2. Images showing the final state of a model test. The structure and ice pile-up are at the centre, the intact ice sheet is to the right and the open water channel to the left with loose ice pieces left behind in the wake as the structure moved from left to right.

3.1.2 Test Setup and Parameters

The model tests selected for analysis were performed in HSVA's large ice model basin. The width of the structure was set to 5.00 m with 1.25 m length of encroachment zone on the top surface of the structure. At the rear part of the encroachment zone, a vertical wall was mounted to avoid ice being pushed off the structure. Model tests were performed in shallow water conditions with the structure mounted to an installation frame resting on a false bottom. The water level was 0.33 m in model scale, while the freeboard was 0.20 m.

The model was constructed on an aluminium frame equipped with four six-component load scales for measurement of ice loads on the structure in the x-, y-, z- directions to determine the rubble weight of the encroached ice and the total force on the structure. Above carriage and underwater video cameras and lights were installed for observation recordings.

All ice encroachment tests were done by pushing the structure through the ice sheet at a speed of 0.026 m/s. Ice strength, ice thickness and freeboard, are shown in Table 3-1. Further details can be found in Bridges et al. (2016).

Table 3-1. Ice model test schedule.

ID	Ice thickness, h_i [mm]	Flexural strength [kPa]	Compressive strength [kPa]	Freeboard [cm]
1010	54.6	83	148	20
1020	56.9	62	110	20
1030	57.4	43	76	20
2010	41.3	72	133	20
3010	55.7	60	115	+30.6

3.1.3 Results from Ice Model Tests

The ice model test results were used for analysis, such as investigating the variation in position of vertex, ice rubble slopes, and correlating these with the forces acting on structure. The process in terms of the different stages and levels of buckling, compressive, upward and downward flexural failure was investigated, as during observations buckling and subsequent flexural failure was observed prior to the end of force chains driving an encroachment event. For example, the ice encroachment process can be analysed by investigating the final piles left after the tests. The clear difference in the pile-up height and extents of ice encroachment can be seen when comparing the tests with varying ice properties, as is clearly shown in Figure 3-3. A marked difference is seen in the ice encroachment height, distance and position of vertex. The slope angle is likewise steeper with the stronger ice. An example of the change in rubble formation is also illustrated in Figure 3-4.

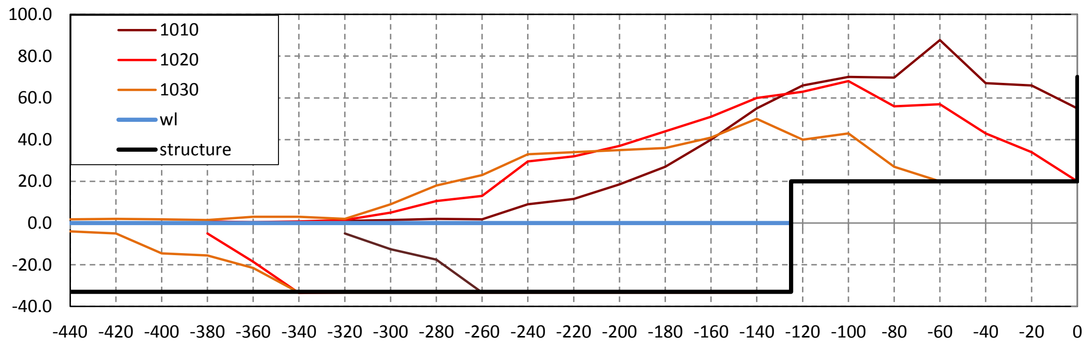

Figure 3-3. Comparison of envelopes of cross section profile measurements for test Series 1010 -1030, with variation in ice strength (1010 high – 1030 low). Increase in the maximum height and encroachment length with increasing ice strength is clearly seen.

Figure 3-4. Cross section photos taken at the end of the ice encroachment model tests with 'soft' and 'strong' ice (right and left image respectively). Layering of ice is clearly evident in the strong ice, whereas soft ice pile is composed of broken and randomly orientated ice.

3.2 Numerical Modelling of IE

The discrete element approach that we used for modelling ice encroachment is based on a model constructed to simulate the ice ridging process in Arctic sea ice. Hopkins (1994) developed a dynamic model of pressure ridge formation, in which an intact ice sheet covering a refrozen lead was pushed at constant speed against a thick multi-year ice floe. The thin sheet, breaking repeatedly in flexure, created the rubble blocks, which form the ridge sail and keel. This work was extended by Hopkins (1998) to perform much longer simulations to determine the evolution of the ridge profile, ridging forces, and energetics as functions of ice thickness and the amount of ice pushed into the ridge. A part of this goal was the determination of maximum sail heights, keel drafts, and ridging forces. The pressure ridging problem has a strong similarity to the problem of ice encroachment if one substitutes a structure and a shallow seabed for the thick multi-year floe. The discrete element modelling approach used here is two-dimensional. It models a vertical slice through an ice sheet and rubble pile. The conclusion of a typical simulation is shown in Figure 3-5.

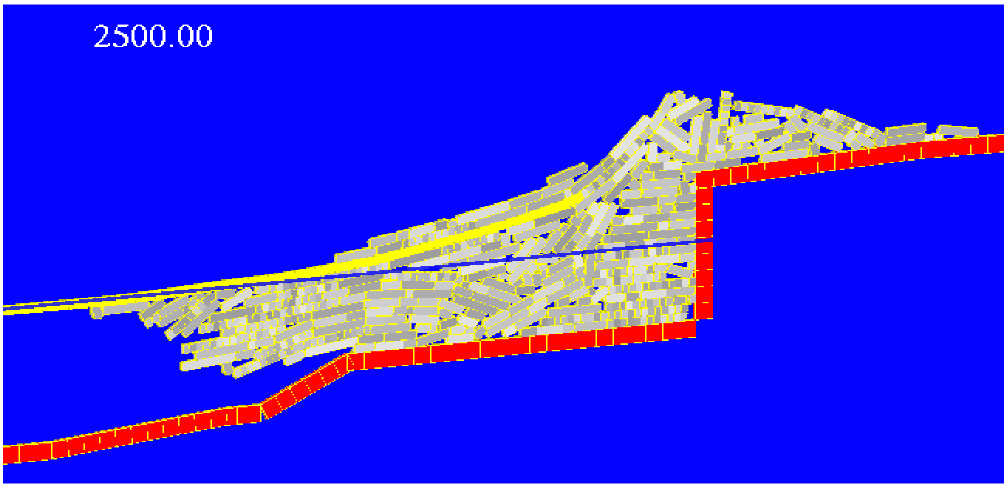

Figure 3-5. Showing the conclusion of a typical 2D simulation. The structure is red, the sheet is yellow, and the ice blocks are grey.

The two-dimensional ice sheet is composed of elements or blocks that are 'glued' together as shown in Figure 3-6. When the sheet bends the faces of adjacent blocks move relative to one another. The viscous-elastic glue that holds them together has a stiffness $k=E/l$ where E is the Young's modulus and l is the width of a block. A tapered viscous damping boundary condition is applied to the sheet to absorb elastic waves travelling toward the left most end of the sheet caused by fracture at the rubble pile. When the stress at the top or bottom of a joint between blocks exceeds the specified tensile or compressive strength a crack is initiated that travels along the joint at a constant speed. When the joint is broken the piece that breaks off the sheet forms a larger rubble block composed of several of the basic rectangular blocks shown in Figure 3-6. This block is added to the rubble pile accumulating at the structure.

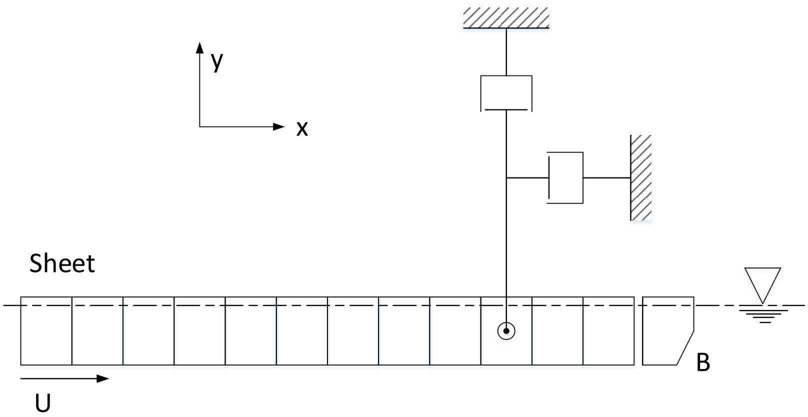

Figure 3-6. Discretisation of the two-dimensional ice sheet into uniform rectangular blocks; showing the viscous damping boundary condition on the ice sheet. The tip of the sheet is bevelled (point B) to facilitate the sheet riding over rubble blocks.

The model's two-dimensionality has several shortcomings that need to be discussed in some detail. In a three-dimensional model ice experiment, when a rubble pile forms against a vertical wall, the oncoming ice sheet pushes the pile against the structure. Because the sheet is wide (several ice sheet characteristic lengths) compared to its thickness it does not usually fail uniformly across its entire width. Instead it fails locally at points where the leading edge of the sheet encounters obstructions and forces are highest. Over time this makes the compression exerted by the sheet on the rubble pile more consistent in the sense that when the sheet fails locally the sheet to either side of the failure zone continues to exert forces through the rubble pile to hold the pile against the wall. As a consequence of this continuous compression the rubble pile in a model ice experiment appears to grow rather smoothly. Furthermore, because the rubble pile is under continuous compression, the pile tends to become higher and steeper than hydrostatic equilibrium and the angle of repose would otherwise permit. In contrast, in a two-dimensional simulation, when the sheet fails compressive forces on the rubble pile are entirely removed and the rubble pile slides away from the wall toward hydrostatic equilibrium. To counter this weakness of the two-dimensional model the viscous drag on the submerged rubble blocks is increased (by several orders of magnitude). This reduces the speed with which the rubble pile collapses toward hydrostatic equilibrium following flexural failure and thereby gives the oncoming sheet time to re-establish pressure on the rubble pile.

In a real three dimensional ice sheet we speculate that before two newly fractured surfaces separate there is some persistent interlocking of the surfaces that allows significant shear force to be transmitted across the fracture. This interlocking allows the real sheet to appear to undergo more extreme bending. The elastic modulus of an ice sheet dictates the degree of bending the sheet will tolerate before breaking in flexure at a given tensile strength. Therefore, to simulate the bending of the three-dimensional sheet in the two-dimensional model the value of the modulus used in the simulations must be significantly reduced. The artificial reduction of the modulus does not strongly affect the energetics of the rubble piling process since more than 90% of the total energy consumed is dissipated by frictional sliding (Hopkins, 1998).Once a block has broken off the sheet it becomes part of the rubble accumulating in front of the structure. As ice is broken off the sheet more ice is added at the trailing end of the sheet to compensate. In Figure 3-5 the ice sheet has built a grounded rubble pile before the structure and used the support of the rubble pile to override the wall. The yellow part is the intact sheet. When blocks break off the parent sheet, the block at the leading edge of the sheet and the block that has just broken from the sheet are bevelled to model the abrasion that occurs in real ice. The appearance of the sheet (yellow) and rubble blocks are shown in Figure 3-7.

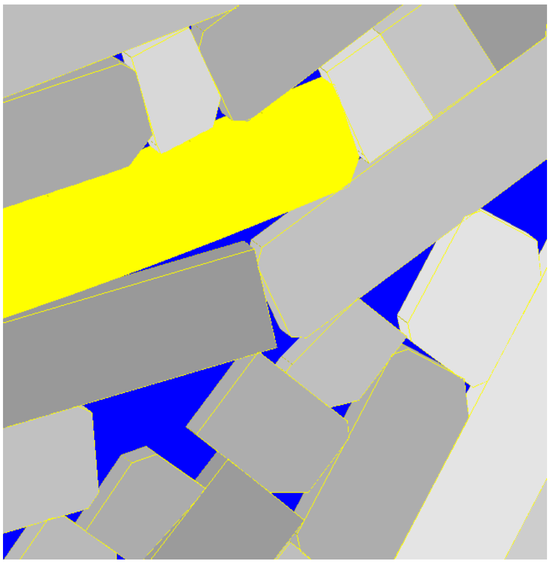

Figure 3-7. Close up image of broken ice pieces during the DEM simulation with the leading end of the ice sheet (yellow) and surrounding blocks broken from the sheet. The bevelling process can be seen which is applied after the ice breaks and models the abrasion of the ice.

3.2.1 DEM Setup and Parameters

We designed a simulation of a vertical faced structure that is based on the Arctic pressure ridging model used successfully in the modelling studies described above. In the model an ice sheet of the specified thickness is pushed against the structure.

At the beginning of a simulation the end of the sheet furthest from the structure starts moving at a speed of 0.05 m/s. The speed increases linearly over the first 400 s of the simulation to a speed of 0.2 m/s whereupon it remains constant. At this speed we consider that the inertial forces are negligible.

The modulus used in the simulations is 100 MPa to minimize brittle behaviour in the two dimensional model. The ice thickness was varied from 0.3 to 0.9 m. The width of the individual blocks that compose the sheet was 1/8 of the characteristic length.

The sheet floats on the water and buoyancy forces on the sheet and blocks are included, but not dynamic pressure effects. When the sheet impacts the structure or ice rubble it bends and fails in flexure. Flexural failure occurs when the tensile or compressive stress at the top or bottom of the sheet exceeds the specified strength.

3.3 Comparison of Ice Model Test and DEM Results

In the following a comparison between the ice model tests and DEM results is presented and discussed. The ice model tests used in the comparison were those that produced significant encroachment and also measured forces and profiles across the transverse extent of the structure.

3.3.1 Test Parameters

The ice parameters are listed in the following Table 3-2 along with the scale factor used . The scaling factors were obtained by dividing the DEM ice thickness; either 600 or 900 mm by the model ice thickness. Ten simulations were performed with each set of input parameters.

Table 3-2. Main parameters from the model tests.

ID	Modulus MPa	Bending strength kPa	Ice thickness mm	Length m	Scaling factor
1010	78	83	54.6	16.4	16.5
1020	42	62	56.9	16.1	15.8
1030	28	43	57.4	16.5	15.7
2010	23	71	41.3	23.7	14.5
2020	14	43	42.2	26.3	14.2
3010	49	60	55.7	16.9	16.2
3020	41	57	57.9	16.1	15.5
3030	24	32	58.2	16.1	15.5

3.3.2 Ice Encroachment Profiles

The profiles of the model test (test 1010) and the profiles of the 10 corresponding simulations are shown in Figure 3-8. Note that the model test profiles have been scaled to full-scale values. The results are seen to be reasonably similar in shape. The extent and average height of encroachment is also similar. The main difference is that the DEM appears to show more rubble ice about 10 to 20 m (in full scale units) from the structure edge.

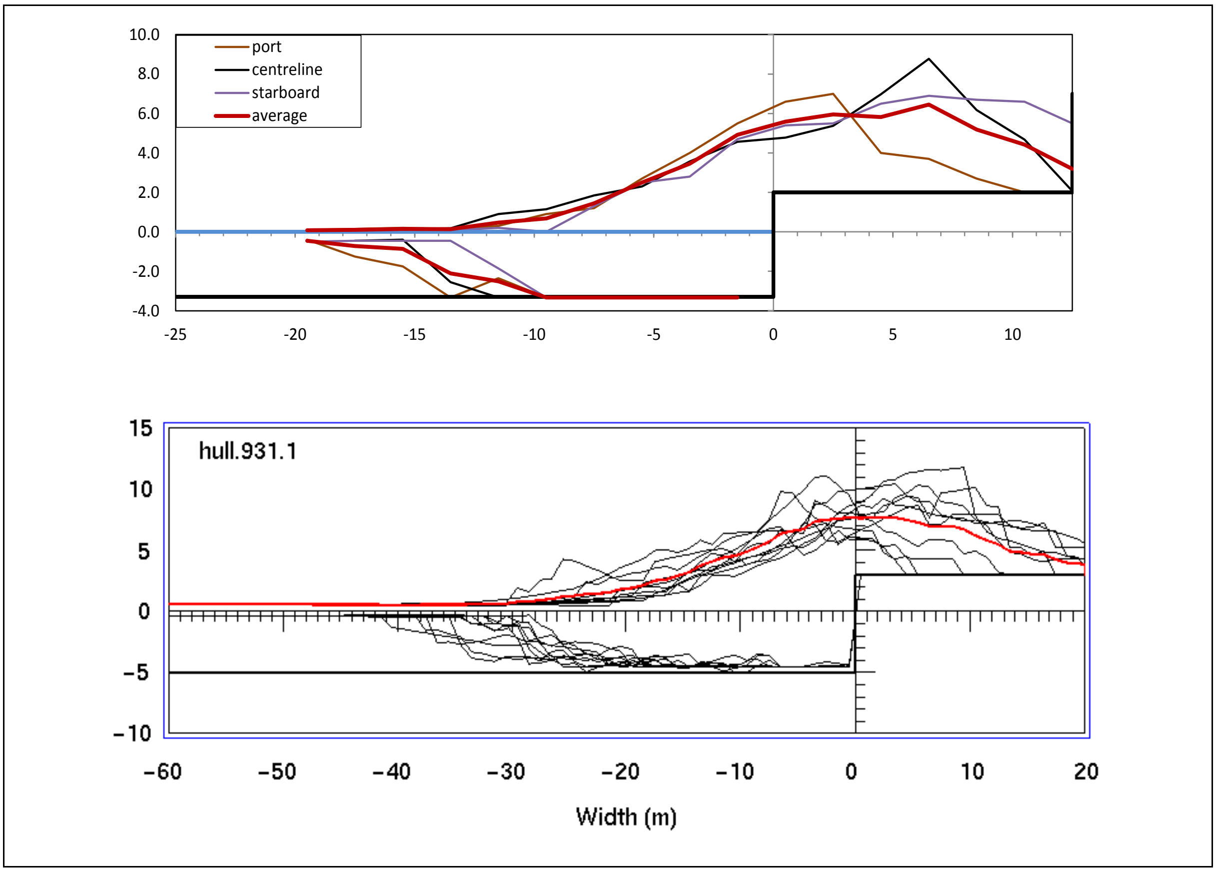

Figure 3-8. Profiles of the ice encroachment piles at end of tests for ice model test 1010 (upper image) and corresponding series of DEM simulations (lower image).

3.3.3 Ice Forces

Two simulations were chosen from the two sets of 10 to compare with model tests 1010 and 2010. The simulations chosen were those that matched the final weight of ice on the structure as closely as possible. The longitudinal and vertical forces from the 1010 model test and the forces from the simulation (9315) are shown in Figure 3-9. It should be noted that the variation in the DEM results can be quite significant, resulting in changes in the order of approx. ±50%, reflecting the variation in IE observed in the profiles shown in Figure 3-8 above.

In Figure 3-9 the *x*-direction force acting on the structure face is red and the *z*-direction force, the weight of the ice on the structure that includes the grounded rubble is blue. The full-scale simulation forces (dimension force per unit width) are scaled by dividing the forces by the square of the scaling factor in Table 3-2 and multiplying the scale force per unit width by the effective structure width. For the *z*-direction force the width is the actual 5 m structure width. However, for the *x*-direction force a width of 7 m is used to account for the extra width of the zone of deformation in front of the structure.

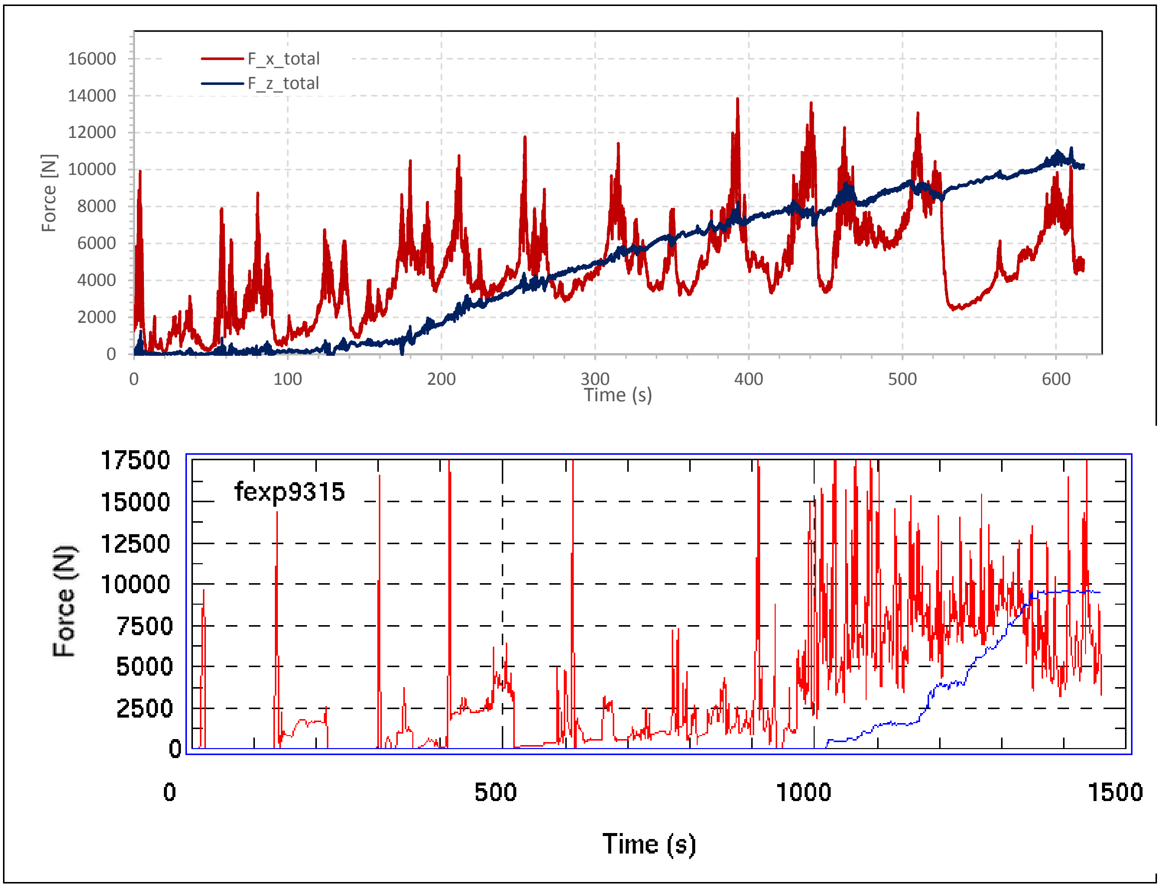

Figure 3-9. Longitudinal (red) and vertical (blue) forces from the 1010 model test and the forces from a corresponding simulation (9315). Similar values in terms of magnitude are observed, however the ice model tests show a smoother progression of longitudinal forces compared to the DEM.

In Figure 3-9 although the forces in the model tests show significant qualitative differences in appearance, they agree quite well in the magnitudes of the peaks. The different appearances may be attributed in part to being a product of the two-dimensionality of the simulations and the three-dimensionality of the model tests. In the three-dimensional model test, when the oncoming ice sheet pushes against the rubble pile and the structure, because the sheet is wide (several characteristic lengths) compared to its thickness, it does not usually fail by bending uniformly across its entire width. Instead it fails locally at points where the leading edge of the sheet encounters obstructions and the stresses are highest. Over time this makes the compression exerted by the sheet on the structure more stable in the sense that when the sheet fails locally the intact sheet beside the failure zone continue to transmit force to the structure. In contrast, in a two-dimensional simulation, when the sheet fails it momentarily loses contact with the structure or rubble pile and the compressive force that it exerts drops to zero. This difference can be clearly seen by comparing the forces in Figure 3-9.

In Table 3-3 the numerical results are compared to the results from the ice model tests. The numbers in the table are scaled values for the simulations using the scaling discussed above. F_Z *max* is the weight of the ice on the structure. The values of F_Z *max* are quite similar for the two pairs of simulations because it was the criteria used to select which simulation from among the set of 10 to compare with the model test. In the 1010/9315 comparison the *x* direction average forces and the work done to create the ice piles are quite similar. However, in the 2010/6316 comparison the *x* direction average force and the work in the model test are almost double the force and work in the simulation. The different appearances of the forces can be seen in Figure 3-9. The reason for the good agreement in one case and the rather poor agreement in the other is attributed to the variability in the 2D model. The work in the ice model tests is computed by calculating the average force from the ice model test data as in Figure 3-9 and multiplying by the length of the sheet. The work scaling uses the 7 m effective structure width.

Table 3-3. Forces and energetics from the comparison between model and DEM.

	Thickness (mm)	<*Fx*> (N)	*Fz* Max (N)	Work (J)
1010 Model Test	54.6	4197	10000	63478
9315 Simulation	900	3925	9598	63189
2010 Model Test	41.3	3269	9000	71909
6316 Simulation	600	1607	9175	38171

3.3.4 IE Progression

The IE progression over time of the simulation and ice model tests were also compared. For example, as shown in the following Figure 3-10. The dash line denotes the ice model test results, and solid line is the simulation results. In general the simulation results show good agreement with the results of model tests, albeit recognising some differences, especially in the initial stages.

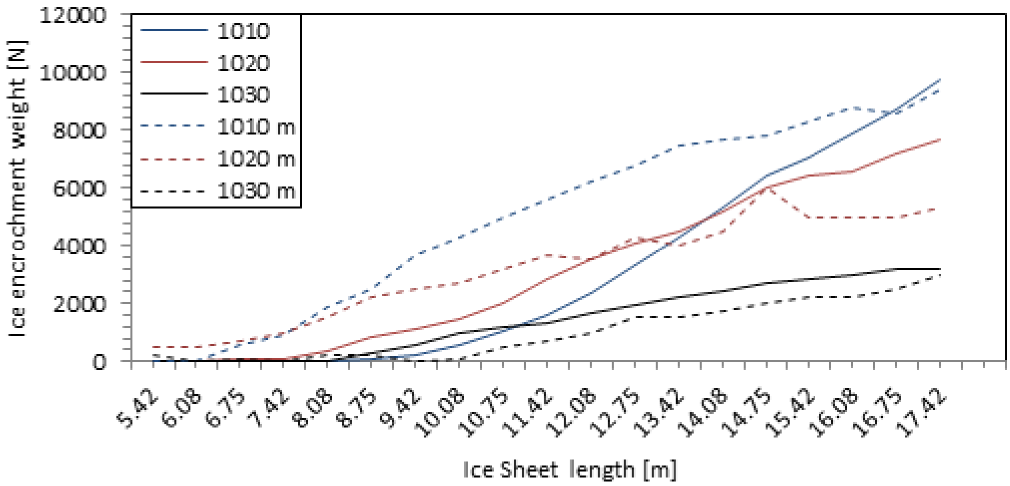

Figure 3-10. Comparisons of the progression of IE with series 1000 model tests and simulations. Solid line represent the simulation and dash line (denoted m) represent the ice model test results. The numerical and model results follow similar rates, although Increase in IE is observed in the numerical scheme compared to the model tests (for 1010 and 1020 tests).

3.4 Comparison of Results with Full Scale IE Events

This section considers the IE events based on full scale data. The data is based on events in the North Caspian Sea which has extensive shallow water and can experience significant ice movements. Ice pressure ridges and rubble piles can be found throughout the North Caspian Sea, especially in the 2 m to 6 m water depth range. There appears to be limited correlation between where grounded features are found from one year to the next. Rubble pile and pressure ridge dimensions vary dramatically, especially for grounded features. Rubble pile heights greater than 10 m have been commonly observed, see Evers (2001). Observations of IE suggests the likelihood increases if the ice extends over large areas of unbroken ice with minimal irregularities. When ice movements occur for many hours it may cause multiple pile ups.

Prior to presenting the results it is worth pointing out differences between ice model tests and full scale data. In the ice pile-up process at full scale there is a time dependent intermittency that allows parts of the ice pile to freeze (and consolidate) in place before another event occurs, whereas in the model tests the ice rubble appears to be quite mobile. There are also hydrodynamic differences between the model tests, where water flow around the edges of the structure is constricted by the tank walls in contrast to the situation in the Caspian were the movement of water may be the same speed as the ice. However, the differences observed in model tests when pushing the ice into the structure and pushing the structure into the ice appeared minimal.

The encroachment events of vertical structures were selected for this study based on Caspian Sea data, for example see Barker & Timco (2017) and Mckenna et al. (2011). In order to compare full scale ice encroachment events with ice model tests, the full scale data were scaled. All the ice thicknesses were scaled to 0.06 m which is equal to the ice sheet thickness in model test series 1000 and 3000. Other data were scaled by the same scaling factor. However the data of full scale events do not contain ice strength and all parameters varied. Hence, we compared the IE height (h_{ie}) and pile height (h_{ip}). We compared these values in relation to the length of ice sheet, L, and also with the ice thickness, h_i. The results are presented in Figure 3-11. The values are similar in full scale events and ice model tests which indicates the ice model tests are representative of full scale events. When the values are normalised with the ice sheet length they give a better correlation than using ice thickness. The differences in the ice model and full scale data may be caused by the uncertainty parameters including ice strength, structure geometries and scaling law.

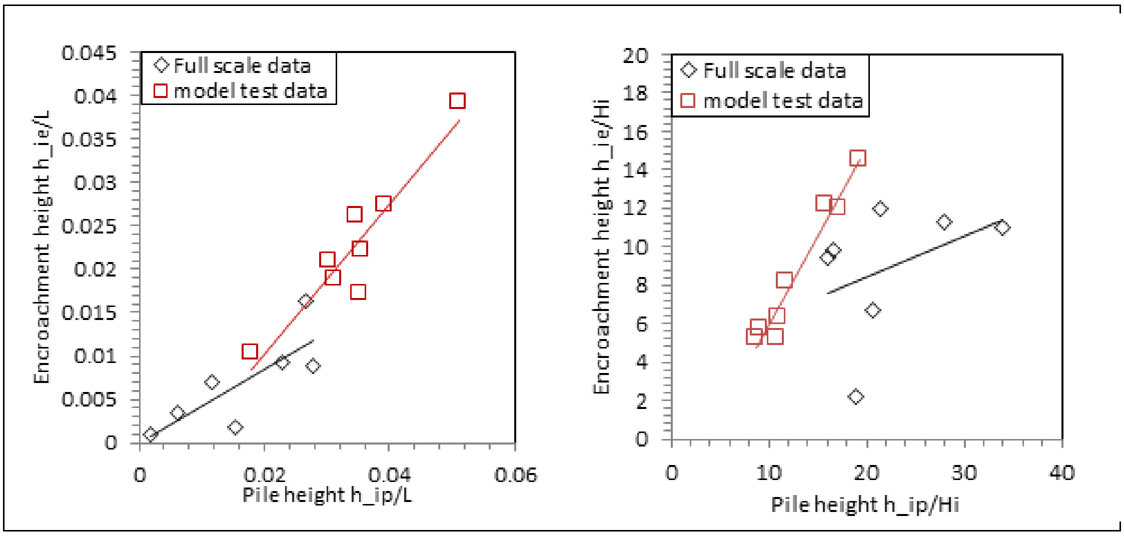

Figure 3-11. Comparison of encroachment height, h_{ie}, and pile height, h_{ip}, for full scale data and model test data. Values are normalised with ice sheet length, L (left image), and the ice thickness, h_i (right image). Linear trend line used as indicative of tendency only. The plots show similarity in the ice model and full scale results, with the normalised values using ice sheet length indicating a better correlation than using the ice thickness.

4. INFLUENCE OF ICE PROPERTIES

The effect of external parameters, i.e. the ice properties, on the susceptibility of IE is investigated in this chapter using the results of the ice model tests and DEM simulations. There exist numerous ice data characteristics that can be input, however for ice encroachment these external parameters are mainly related to the ice cover and are discussed in the following sections.

4.1 Ice Drift Length and Incidence Angle

The drift length refers to the length of the ice cover available to impact on the structure. Often the length in itself is not decisive as the driving force (wind) direction changes before all the potential ice has impacted the structure; more important may be the duration of the encroachment event together with the drift speed. The main effect of the drift length is to increase the size of the rubble pile. Occurrence of ice encroachment requires a pile height up to the freeboard and a relatively shallow slope angle. Thus the geometry of the pile in front of the structure (shape and water depth, freeboard height) determines how much ice (drift length x ice thickness) is needed to start an ice encroachment event. For example, using typical freeboard heights and water depths for Caspian Sea developments, the required cross sectional area of ice encroachment pile is roughly 150 m^2, meaning a drift length of 300 m of 0.50 m thick level ice, neglecting porosity. Also important is the incidence angle which refers to the angle between the ice drift direction and the structure side tangent line. Thus if the drift is normal to the structure side, this angle is 90^0. If this angle is small, the ice drifting against the structure just slides along the wall.

4.2 Ice Thickness and Mechanical Properties

Increasing ice thickness reduces the drift length required to create a pile of a given volume. Thinner ice has a tendency to raft rather than rubble. In two ice sheets slide over each other diminishing the likelihood of ice encroachment. The range of ice thickness where rafting prevails is unknown, but no ice encroachment has been observed in the Caspian Sea with ice thinner than 0.2 m (for vertical structures). The difference in IE from results in the simulation due to ice thickness is shown in Figure 4-1.

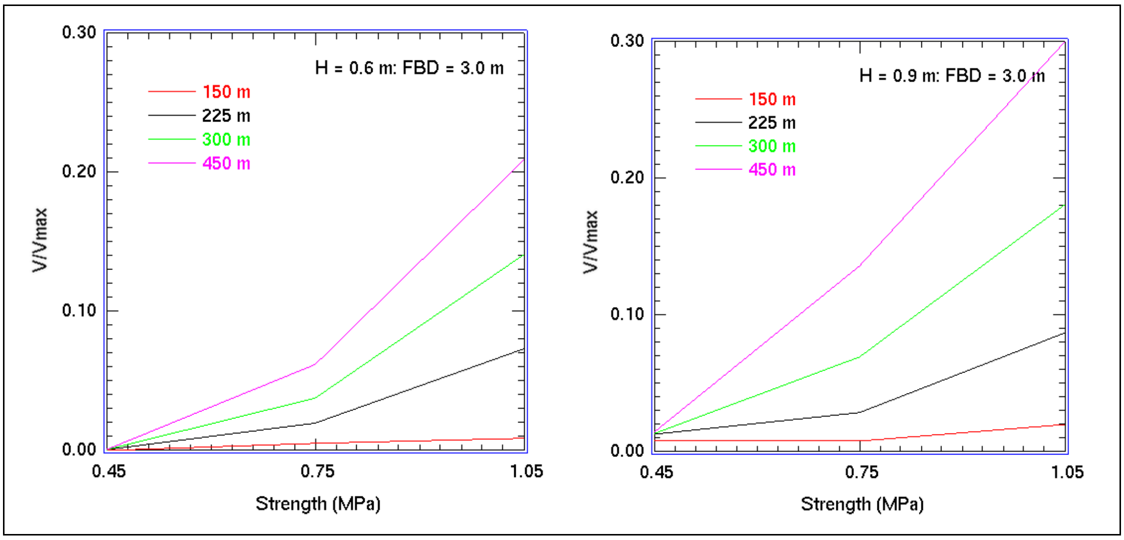

Figure 4-1. Encroachment volume (from DEM) as a function of ice thickness and strength. Left image is ice thickness 0.6 m and right image is ice thickness of 0.9 m. V/V_{max} is the fraction of total ice push that ends up on top of the structure, i.e. the volume of ice from the ice sheet and the volume of ice that has encroached on the structure. Increase of IE is observed with increase in ice thickness and also ice strength.

In the model tests increased ice strength led to increased ice encroachment. As noted earlier, low model ice strength caused the rubble pile in front of the structure to grow horizontally, rather than vertically. The reason for the absence of vertical build-up may be the low compressive strength, along with an associated reduction in bending strength and Young's modulus, i.e. stiffness change, that inhibits force chains from forming that in turn reduces the ability of the oncoming ice sheet to push ice blocks up the rubble pile onto the structure. Ice strength is measured by the compressive strength and bending strength. If ice is weak in compression, no force chains can form and no ice encroachment occurs. Ice fails at the pile, without upwards pile-up occurring, increasing the seaward extent of the pile in front of the structure. The effect of bending strength is more complicated and model testing where bending strength was varied did show some effect of bending strength, but this may be caused by weak compressive strength as bending strength cannot be changed in model tests individually. In numerical simulations stronger ice in bending strength showed more ice encroachment. Thus it can be concluded that in general stronger ice shows more ice encroachment.

5. OBSERVATIONS OF IE PROCESS

In this section we discuss the IE process based on the observations of the DEM simulations and ice model test data to gain particular insight into the ice interaction mechanisms and ice encroachment piles.

5.1 IE Geometry

The slope angles of the IE piles shown in Figure 2-3 were measured in the ice model tests . The results in Figure 5-1 show the rubble and IE angles α_{fs} and α_{es} range from 10° to 30° with the increase of bending strength, while back slope α_{bs} varies from 20° to 45°. Thus, the rubble front angle α_{fs} may be considered to be quite constant, whilst the pile-up angle α_{es} is clearly related to the strength. The back slope angle α_{bs} shows significant variation, however this may be attributed to the influence of the rear barrier wall. A further parameter in the IE piles is the vertex position, and results show the change with bending strength is clearly seen, as in Figure 5-2. This supports the supposition that the ice strength influences the IE process.

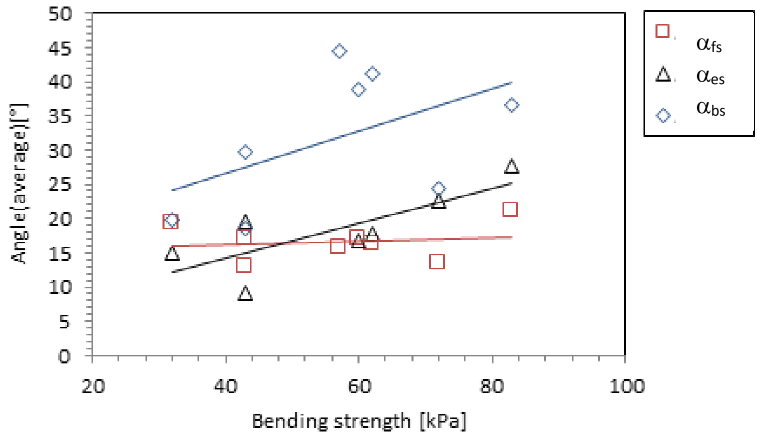

Figure 5-1. Relationship of angle and bending strength (Angle 2 is the rubble front slope, Angle 3 the IE front slope, and Angle 4 is the back slope). Linear trend line used as indicative of tendency only. The front and back slope are seen to change with variation of ice strength, becoming steeper, although the front rubble angle remains reasonably constant.

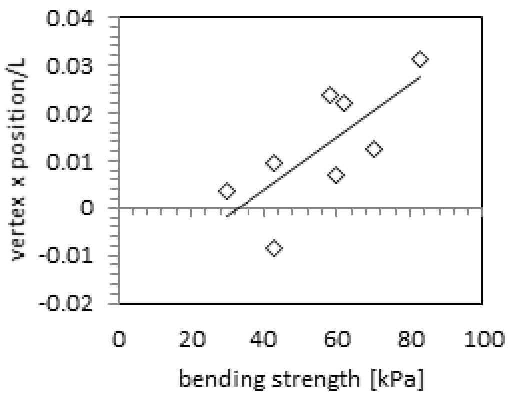

Figure 5-2. Relationship of vertex position and bending strength for ice model test results. Where L is the length of ice sheet. Linear trend line used as indicative of tendency only and shows movement of vertex with increase of ice strength. Note, vertex position is in relation to the structure edge, which is set to zero.

5.2 Maximum Pile Height

The amount of encroachment on a structure depends on the ability of the ice sheet to push ice up the pile that forms in front of the structure. The main factors that determine the maximum height of the ice pile-up are ice thickness, bending strength, and freeboard. Ice thickness and bending strength directly affect the strength of the sheet. The stronger the sheet, the higher and farther it can push the ice and the larger the pile that it can create. Ice encroachment depends on first filling the space in front of the structure to create a platform and a ramp to support the sheet while it pushes ice up the pile onto the structure. As the freeboard is increased the volume of ice that is required to fill the space in front of the structure increases. If we assume that the angle of inclination of the pile is the same regardless of freeboard, then the volume of ice in front of the structure increases with the square of the freeboard height.

The factors we considered that might determine the maximum height of the ice pile-up are ice thickness, bending strength, and freeboard. Using the same DEM parameters as above, we performed 10 simulations with each set of values of thickness, bending strength, and freeboard. In all cases the same length of ice, 462.5 m, was pushed at the structure. The maximum pile height in each set of simulations is listed in Table 5-1 below. The maximum height of the encroachment for h = 90 cm and σ_f = 1050 kPa is approximately WL+16 m. The maximum height attained for h = 60 cm is approximately WL+11 m. Interestingly, while the maximum height depended strongly on thickness and strength it was relatively independent of freeboard.

Table 5-1. Variation of the maximum height with ice thickness and bending strength.

Ice Thickness (cm)	Sigma_f (kPa)	Maximum Height (m)
30	450	1.5
30	750	5
30	1050	6
60	450	3
60	750	9.5
60	1050	11
90	450	5.5
90	750	13
90	1050	16

The lack of dependence on freeboard was illustrated by running simulations using 90 cm ice with σ_f = 1050 kPa at freeboard heights ranging from 3 m to 10 m. Ten simulations were run at each freeboard. While the volume of ice encroachment decreased enormously over that range, the maximum pile height remained roughly constant. Put another way, a 13 m pile forms on top of a 3 m structure, while a 6 m pile forms on top of the 10 m structure. Figure 5-3 sketches the concept. While the maximum pile height appears to be independent of freeboard the volume of encroachment is not. This is shown in Figure 5-4.

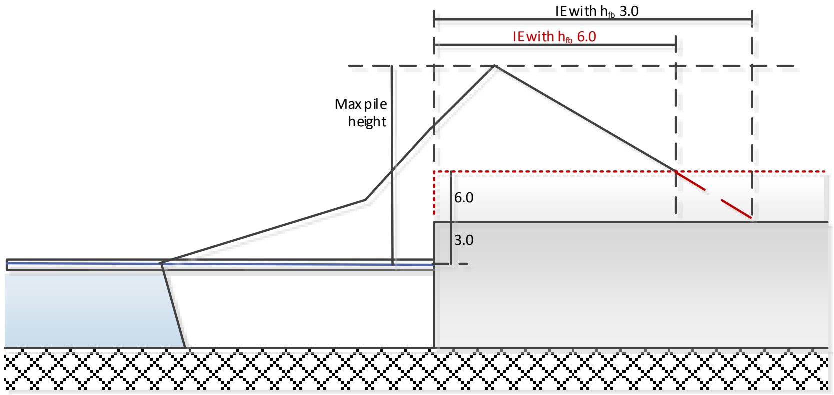

Figure 5-3. Concept of maximum IE height with variation of freeboard (3 & 6 m) resulting in IE reduction.

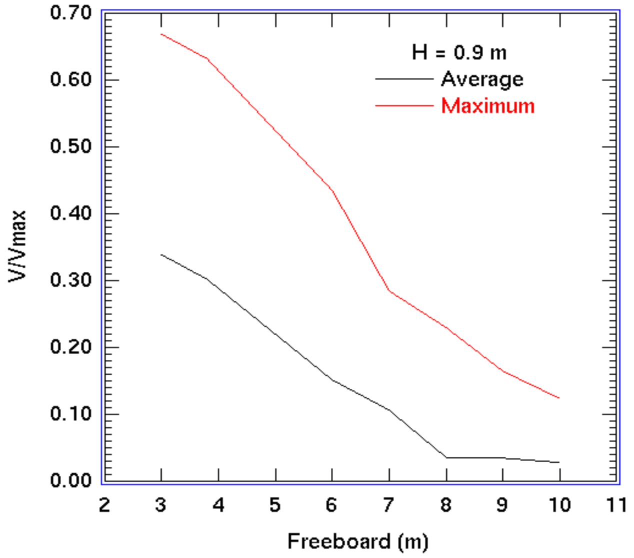

Figure 5-4. The average and maximum encroachment versus freeboard for 90 cm ice. V/V_{max} is the fraction of total ice push that ends up on top of the structure. Decrease of IE is clearly seen with an increase of structure freeboard height.

Furthermore, we expected ice-ice friction to affect the force required to push a train of ice blocks up the face of the pile and thus affect the height of the entrainment pile. A value of 0.3 was used in all of the simulations discussed above. We also tested friction coefficients of 0.2 and 0.45. Interestingly, both produced a slight reduction in maximum pile height. Both sets of 10 simulations were performed at a 7 m freeboard height. The reasons for this are not entirely evident. This may be either a numerical artefact of the DEM simulations or there may be an underlying physical process, and requires further investigation to determine the influence.

Based on the results of the simulations we observe that the maximum pile height:

- depends strongly on ice thickness and bending strength.
- is relatively independent of freeboard height.

- is relatively insensitive to the ice-ice friction coefficient within the range 0.2 to 0.45.

We should emphasize that while the maximum pile height does not depend on freeboard the volume of encroachment does. A given maximum pile height implies a large encroachment volume above a low wall and a small encroachment volume above a high wall. However, there is also a more subtle secondary effect of freeboard on potential ice encroachment. This follows from the fact that for encroachment to happen the area in front of the structure must be filled with ice rubble to support the ice pushed onto the structure to form the pile. If we assume that similarity exists between the rubble piles with respect to the differing freeboard heights then the volume that must be filled increases as the square of the increase in the freeboard. Increasing freeboard requires a greater volume of ice rubble to fill the area in front of the structure that requires a greater extent of ice sheet be pushed into the rubble pile. The probability of occurrence of an ice push of a given length must decrease with the increase in length. Therefore, increasing the freeboard height might reduce the probability of IE due to the reduced probability of occurrence of the required ice extent and movement.

5.3 Equal Ice Volume Concept

In all of the earlier simulations with 30, 60, and 90 cm thick ice the ice speed was constant and the duration of the simulations was 2500 s. This means that the ratio of ice volumes in the simulations was 1:2:3. However, the volume to be filled in front of the structure is the same in each case (under the similarity assumption). So perhaps the 30 and 60 cm ice sheets do not have equal opportunity to cause encroachment. To examine this question we repeated the 60 cm simulations with a duration of 3750 s to increase the ice pushed to the same volume as for 90 cm thickness. One of the simulations is shown in Figure 5-5. The additional ice resulted in a minimal increase in the maximum pile height and encroachment. So while the total ice volume is now the same as in the 90 cm case the maximum pile height is still about 11.5 m, while the maximum height in the 90 cm case is about 16 m. So increasing volume of ice in the 60 cm test to the volume used in the 90 cm test produced no increase in IE or maximum height.

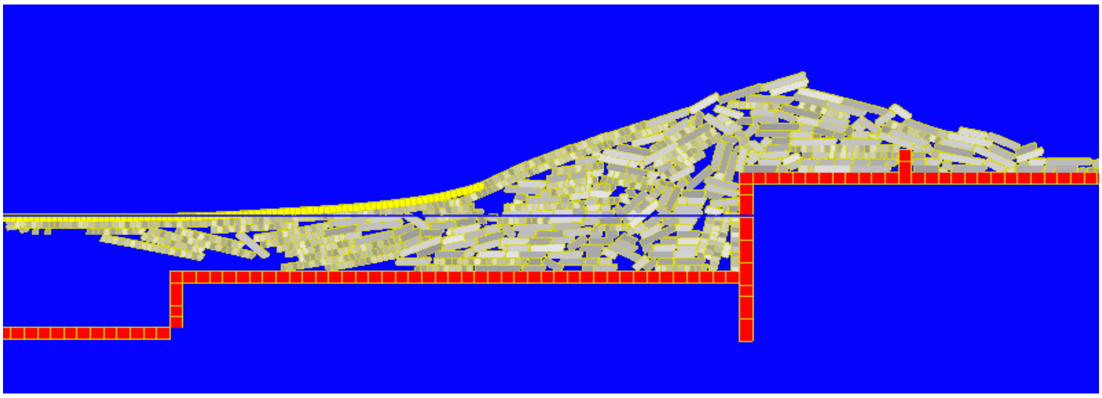

Figure 5-5. A simulation with h = 60 cm at a point when 693.8 m of ice has been pushed into structure. The maximum height is 11.8 m above the waterline.

However, this leads to an interesting thought experiment. If we make the strength of the 60 cm ice the same as the 90 cm ice would that increase the encroachment to the volume found in the 90 cm cases? To check this, we begin by trying to match the deflection of the 90 cm ice under a given load, *F*. The equation for the deflection δ of a cantilever beam of length L is $\delta = FL^3/3EI$, where E is the modulus and I is the moment of inertia. To obtain equal deflection we find that the modulus of the 60 cm ice sheet must be increased by 3.375. We also need to match the bending strength so that a

60 cm beam of equal length breaks at the same load. The equation for bending strength is $\sigma f = 6FL/bh^2$, where h is the ice thickness and b = 1 is the out-of-plane unit thickness. Therefore, for the 60 and 90 cm beams to break at the same force, the bending strength in the 60 cm sheet must be 2.25 times greater than in the 90 cm sheet. If we make these changes and rerun the 60 cm simulations for 3750 s we find that, indeed, the encroachment increases and the maximum pile height increases to the height reached by the 90 cm ice sheet. This supports our hypothesis that it is ice strength that controls IE and maximum height.

5.4 Unequal Ice Strength

In all of the earlier simulations we used the same values of bending strength to limit upward and downward bending. However, in the ice model tests and in the field it is likely that upward and downward bending strengths aren't equal. When bending strength is measured in the laboratory and in the field it is generally downward bending strengths that are measured. It is likely that since the bottom of the sheet is submerged and thus warmer than the top of the sheet that is exposed to the air that upward bending strength is less than downward bending strength. Therefore, we ran two sets of simulations to investigate this. In the first set of simulations we fixed the downward bending strength at 1050 kPa and reduced the upward strength by 25% and 50%. In the second set of simulations we fixed the upward bending strength at 1050 kPa and reduced the downward strength by 25% and 50%. We then analysed the volume of ice encroachment produced in each case.

As before the data points are the average of ten simulations. We compared the effect of the reductions on the volume of encroachment at 60 and 90 cm ice thicknesses. Results for 60 cm ice thickness are shown in Figure 5-6. The results show that in all cases the weakening produced some reduction of encroachment and weakening the bottom of the sheet caused more reduction than weakening the top.

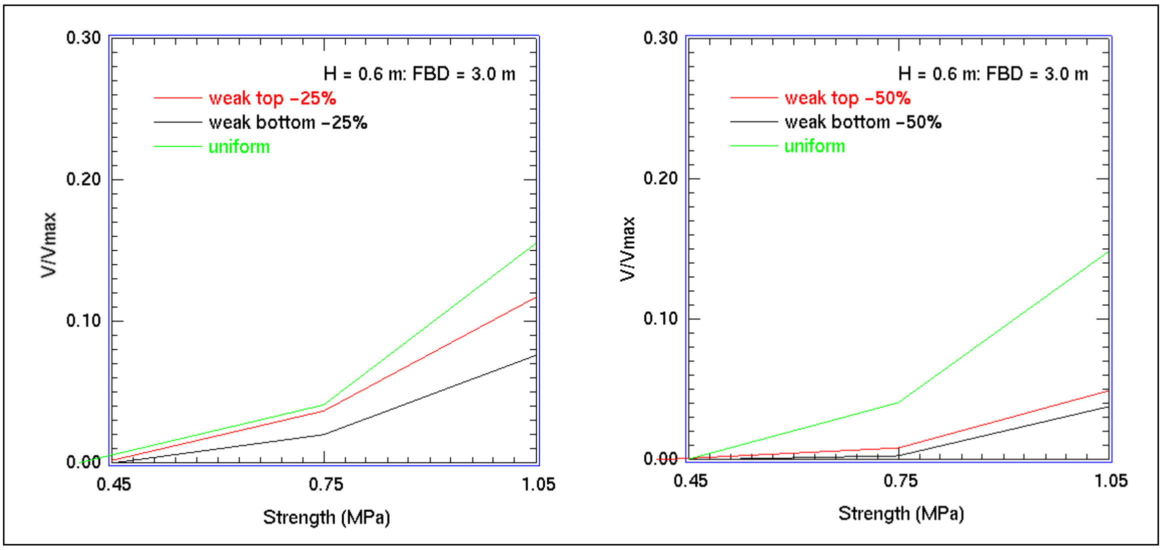

Figure 5-6. DEM simulation results with variation of the top and bottom strength of the ice sheet. Left image shows change of strength by 25% and right image a further increase change of 50%. V/V_{max} is the fraction of total ice push that ends up on top of the structure. Weaker top and bottom strength both lower the IE.

5.5 Influence of Buckling Process on IE

Once the rubble ice has grounded the ice rubble blocks are observed to form from flexural failure of the ice sheet. The blocks broken from the sheet may form a continuous chain of ice blocks that are then pushed up the rubble pile. As the chain lengthens frictional and gravitational forces increase. Eventually the increasing forces exceed the strength of the oncoming ice sheet and another buckling event occurs in front of the rubble pile, as illustrated in Figure 5-7.

It is importance to note that the buckling failure, be it by single or double hinge failure (often seen with two hinges with a large first break and smaller second), has a failure point that is a distance away from the edge of the ice rubble and that of the ride-up ice pieces. So on continuation after a buckling event, the contact with the ice pieces with the ice sheet is lost, breaking the force chains, with the ice sheet then sliding over first the ice broken during buckling then over the ride-up ice pieces. Thus creating a new ride-up event.

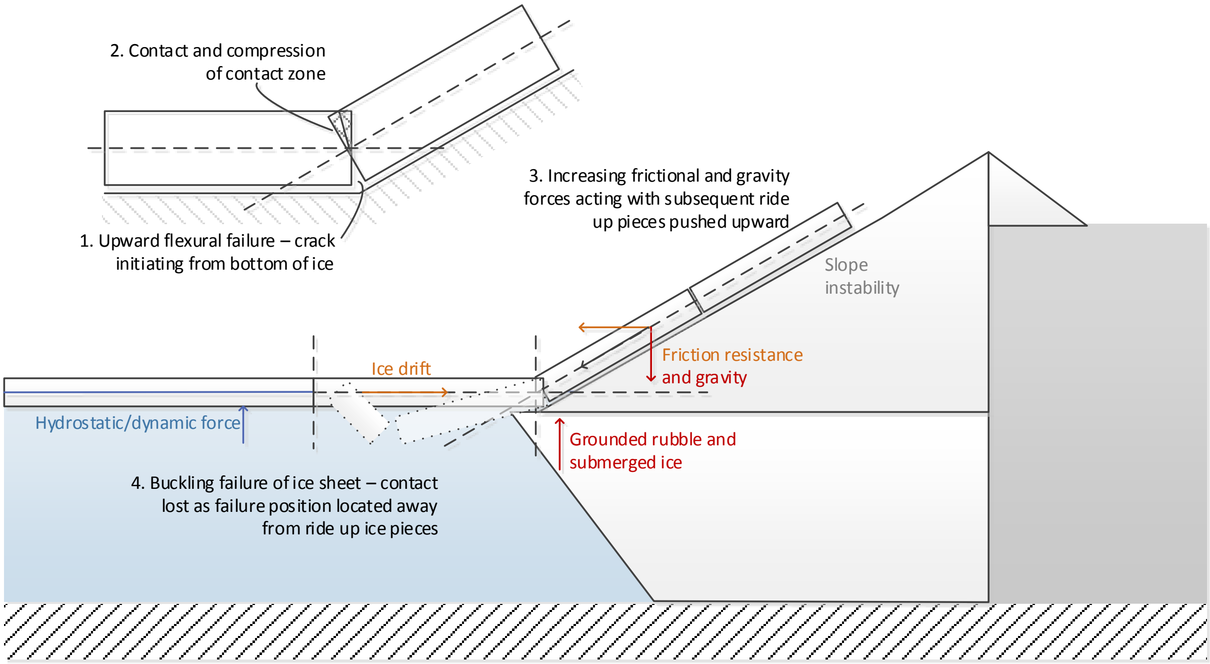

Figure 5-7. Illustration of ice failure processes in ice encroachment (not to scale).

In this process, the rubble angle plays a significant role. A steeper angle, i.e. observed in initial stages, creates greater downward force, thus pushing the ice sheet downwards and submerging it. With milder slopes there is a greater horizontal component of the resistance force, and thus greater compressive loading resulting in buckling. The compressive strength of the ice sheet influences the compaction of the ice rubble, until with sufficiently high compressive strength the ice sheet is able to penetrate into the rubble pile.

As the IE process continues the size and height of the pile atop the structure increases. The pile atop the structure is a continuation of the pile in front of the structure. The force resisting the oncoming sheet is proportional to the height of the entire pile from the waterline to the top of the pile on the structure. As the height of the pile grows so does the force. The force is transmitted through the chain of blocks pushed up the pile all the way back to the intact sheet. Once the force transmitted through the sheet reaches the buckling strength of the sheet, then the sheet will buckle.

At this point we need to introduce the topic of non-simultaneous failure. Non-simultaneous failure of an ice sheet means that, across the width of the leading edge of the ice sheet, failure is occurring at some points and not at others. When watching a ride-up event occurring one notices failure occurring sporadically at one point or another and then ride-up continuing as the sheet overrides the previous failure zone. Figure 5-8 shows a time series of buckling events that occurred during an ice model test that were compiled from a video taken from above the sheet. The arcs in the figure show the extent of each buckling event. The length of the arcs show that the buckling events did not happen across the entire sheet. Eventually, the size of the ice pile in front of and on the structure is enlarged to the point where it is too difficult for the ice sheet to push more blocks onto the pile. The final stage of the encroachment process is reached when the pile can grow no higher. As the ice sheet continues to move toward the structure the ice rubble will accumulate in front of the pile and the pile will grow in the direction of the oncoming sheet.

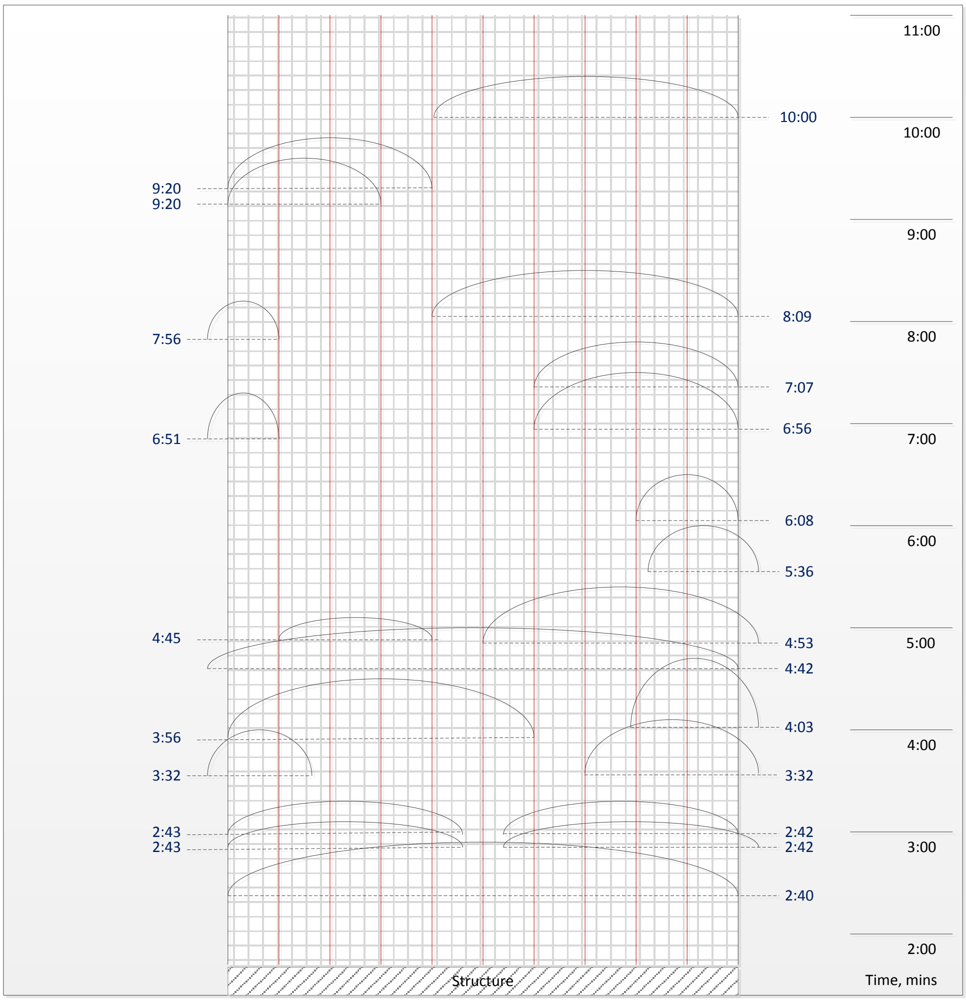

Figure 5-8. Failure process observations during ice model tests. Bird's eye view with failures shown (black arcs) over the width of structure (red lines). Start of test is at base of figure and increasing time moving upwards (black text) and the specific times of buckling events (blue text).

To investigate this process, the buckling forces of all model ice tests were calculated using Hetenyi, (1946) and the following equation: $F_b = \alpha \rho_w g B L_c^2$ where L_c= characteristic length $[Eh^3/(12\rho_w g)]^{1/4}$. The peak buckling force and number of peaks are plotted in

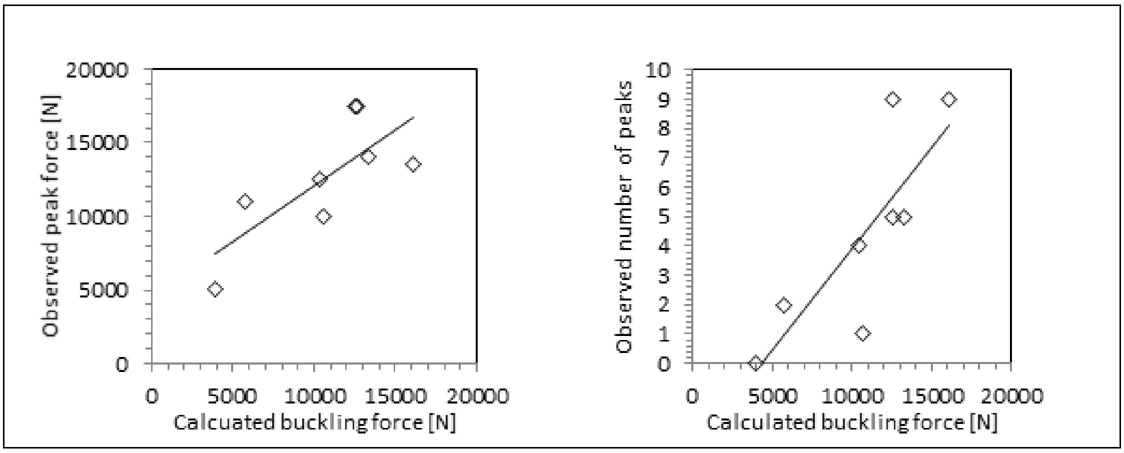

Figure 5-9. The results show that higher buckling force causes more ice encroachment and larger horizontal peak force, and in addition, the number of the peak forces (which are above 10,000 N) increases. A supplementary comment is noted here that the influence of buckling failure for grannular vs. columnar ice may also change the failure process, e.g. pile penetration, piece size variation, etc. This aspect and the effect of buckling strength on IE requires further research.

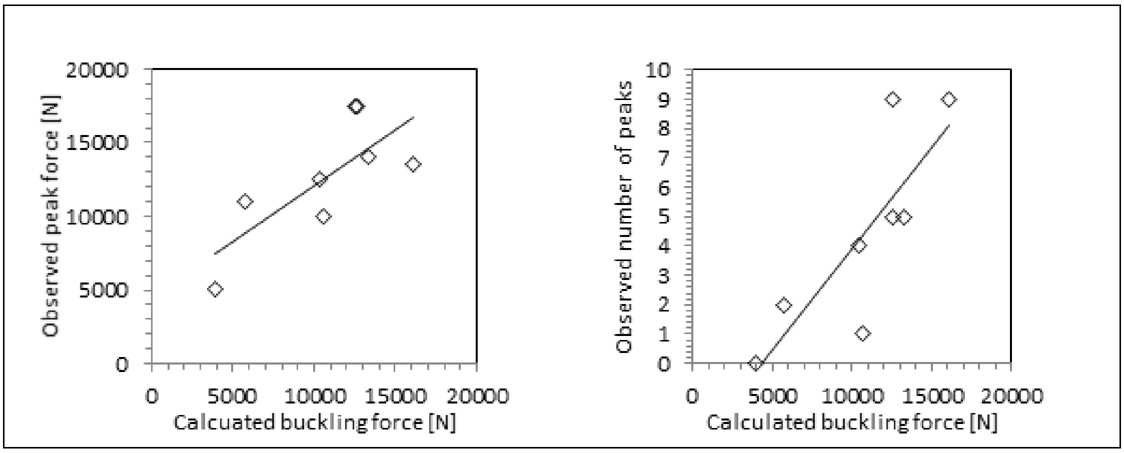

Figure 5-9. Calculated buckling force and the observed buckling peak force during the ice model test (left image) and the observed buckling event frequency greater than 10000 N during the ice model test (right image).

6. EFFECT OF DESIGN PARAMETERS ON IE

In the final chapter, we consider all of the data and results and how the IE process can be influenced by the structure design and the effect of design parameters on the susceptibility and amount of the ice encroachment.

6.1 Water Depth

Once the rubble pile has formed in front of the structure, the water depth does not play any role as the encroachment occurs by ride-up on the slope created in front of the structure. Therefore, the water depth influences the ice encroachment only by how much ice is required to form the grounded pile in front of the structure. For deeper water more ice is required to form this rubble pile, and thus greater a length of ice is required (for the same ice thickness), which implies a longer ice drift duration.

6.2 Freeboard Height

The freeboard height has two types of effect. Firstly with a higher freeboard, more ice is needed to create a rubble front slope enabling ride-up to reach the platform top surface. Thus with higher freeboard, longer drift length is needed. The second effect is to restrict the ice encroachment, as the sum of freeboard height and the height of the ice pile on top of the structure depends on ice thickness (assuming constant ice strength in some specified sea area). Thus if the freeboard is larger, the pile on top of the structure is smaller.

6.3 Slope Inclination

A relatively small inclination is required to enable ice ride-up on an inclined structure without initial creation of a rubble pile; we estimate a slope angle less than roughly 1:4 is required to create a ride-up. Thus if the structure side slope is steeper than this, ice ride-up does not occur until a pile is formed. Only when the pile is large enough to allow a gentle slope to form can ice ride-up leading to ice encroachment happen. .

6.4 IE Protection Methods

There are several ways to decrease the amount of ice encroachment or mitigate its effects. The basic approach is to design the structure considering the combination of the freeboard height with an ice encroachment zone width on top of the structure. As the pile height on top of the structure depends on the freeboard height, also the ice encroachment length depends on it. Thus with higher freeboard, a narrower ice encroachment zone is required. This 'geometric design method' is, however, not very practical nor cost effective. Thus the best way is to consider alternative approaches and tune each alternative with respect to others so that the probability of ice encroachment can be minimised. It is also worth noting that IE also impacts on logistics and access arrangements and that the direct forces associated with encroached ice are typically much less than the direct ice loads (in crushing or flexure).

An alternative to prevent ice encroachment is to build ice protection barriers or structures. Rows of single piles have been tried as well as solid caissons. However, these can interfere with the shipping and logistics, making access to the platform more difficult. Larger ice barriers can also be expensive and thus solutions using intermittent smaller barriers have been tried. Structures designed to break and displace ice sideways to lessen the encroachment have been suggested, but not yet applied. However, even if barriers are used, some ice encroachment zone should be considered as a necessary precaution.

A third method to mitigate the effect of ice encroachment is to build some ice deflectors or walls. These are located at the corner of the structure with the aim to deflect ice that is riding up back toward the rubble pile. The effect of these deflectors is to make the pile required for ice encroachment larger and thus more drift length is needed. Another type of 'deflector' is a solid wall or walls on top of the structure. If the wall is set back from the edge of the structure then it creates an ice encroachment zone.

7. SUMMARY

Ice encroachment is one of the main ice engineering design considerations for artificial islands in shallow ice covered waters and modelling of the ice ride-up and pile-up is necessary for safe and efficient design. Physical control of ice pile-up and ice encroachment is a complex process. This paper provides some results of ice model tests and DEM simulations of ice encroachment that have been carried out. During the physical and numerical testing several different ice and structural parameter values were tested. The results from ice model tests indicate that the strength can to a certain degree be controlled, although it is difficult at the same time to have the correct ice compressive strength, which is an important factor in modelling the encroachment process. Based on the results we can make the following observations:

- The simulations replicate the ice rubble profiles well for a given set of parameters.
- The simulations and model tests have similar peak forces magnitudes.
- For a given ice bending strength and thickness the pile height grows asymptotically to a maximum pile height.
- Maximum pile height depends strongly on ice thickness and bending strength.
- The volume of encroachment is strongly dependent on bending strength and ice thickness.
- Maximum pile height for a given ice thickness and strength seems to be relatively independent of freeboard height.
- The volume of encroachment is strongly dependent on freeboard height.
- Maximum pile height is relatively insensitive to the ice-ice friction coefficient within the range 0.2 to 0.45.
- Once the maximum pile height is reached then subsequent deformation enlarges the rubble pile in front of the structure in the direction of the oncoming ice sheet.
- Simulations give equivalent results at model scale and full scale.

Furthermore, a final conclusion for reliability of any model testing method is given by feedback from nature. Thus full scale observations are extremely valuable. Further information in this field will greatly assist in the development of a realistic numerical and ice model testing of the ice ride-up process and would allow for design and evaluation of advanced ice control measures. It is vital to take proper account of the role of ice properties in ice encroachment events, including the varied physical factors which can influence the ice build-up process. The insights from the study allow the development of technology and knowledge for effective and efficient structures while ensuring personal and platform safety, for operation in ice conditions.

ACKNOWLEDGEMENTS

The authors would like to express their thanks to Salauat Alzhanov, NCOC, and also to Paul Verlaan, Shell, for their support and valuable insights into the ice conditions and events in the Caspian Sea. The cooperation and assistance of Christian Schroeder and the Arctic Technology team at HSVA in performing ice model tests is also appreciated.

REFRENCES

Allen J.L. 1970. Analysis of forces in a pile-up of ice. National Research Council, Ottawa, Canada. Technical Memorandum 98. pp 49-56.

Allyn N. and Wasilewski B.R. 1979. Some Influences of Ice Rubble Field Formations around Artificial Islands in Deep Water. Port and Ocean Engineering Under Arctic Conditions, Norway. POAC79 V1. pp 39-55.

Barker A., Timco, G. and Sayed, M. 2001. Three-Dimensional Numerical Simulation of Ice Pile up Evolution Along Shorelines. Proceedings Canadian Coastal Conference. pp. 167-180.

Barker A. and Timco G. 2007. Modelling Rubble Field Development at Isserk I-15 and its Implications for Engineering Ice Rubble, Proceedings of the 22nd International Conference on Port and Ocean

Engineering under Arctic Conditions, POAC-07, Dalian, China, June 27-30.Dalian University of Technology Press. pp 485-496.

Barker A. and Timco G. 2016. Beaufort sea rubble fields: Characteristics and implications for nearshore petroleum operations. Cold Regions Science and Technology 121. pp 66–83.

Barker A. & Timco G. 2017. Maximum Pile-up Heights for Grounded Ice Rubble. Cold Regions Science and Technology 135, pp 62-75.

Bridges R., Riska K. and Schroeder C. 2016. Model Tests for Ice Encroachment and Formation of Rubble Ice, Proceedings of the 23rd IAHR International Symposium on Ice.

Christensen F. 1994. Ice ride-up and pile-up on shores and coastal structures. Journal of Coastal Research 10-3, 681-701

Coche E. and Kalinin A. 2013. Yamal LNG: Challenges of an LNG port in Arctic. Proceedings of the 22nd International Conference on Port and Ocean Engineering under Arctic Conditions, POAC13-172, 11p.

Croasdale K. M. 1978. Factors Governing the Ice Ride-Up on Sloping Beaches. The 5th IAHR-Symposium on Ice Problems. Sweden.

Croasdale K.R., Cammaert A.B. and Metge M. 1994. A method for the calculation of sheet ice loads on sloping structures. IAHR International Symposium on Ice. International Association of Hydraulic Engineering and Research. pp. 874–885.

Croasdale K.R. 2012. Ice rubbling and ice interaction with offshore facilities, Cold Regions Science and Technology 76–77 (2012) pp 37–43.Crocker G., et al. 2011. Observations of Ice Features in North Caspian, Proceedings of the 21st International Conference on Port and Ocean Engineering under Arctic Conditions.

ElSeify M.O. and Brown T.G. 2006. Formation, Behaviour and Characteristics of Ice Rubble Pile-Up and Ride-Up on a Cone. Proceedings of the 18th IAHR International Symposium on Ice. International Association of Hydraulic Engineering and Research. pp 201-208.

Evers K.U. 2001. Ice Model Testing of an exploration platform for shallow waters in North Caspian Sea. Proceedings of 16th International Conference on Port and Ocean Engineering under Arctic Conditions, Ottawa, Canada, Vol 1, pp. 254-264.

Evers K.U. and Weihrauch A. 2004. Design and Model testing of Ice Barriers for Protection of Offshore Structures in Shallow Waters during Winter. 17th International Symposium on Ice, Saint Petersburg, Russia, 21-25 June 2004. International Association of Hydraulic Engineering and Research. 10p.

Goldstein R., Onishchenko D. and Osipenko N. 2013. Grounded Ice Pile-Up. 2D DEM Simulation. Proceedings of the 22nd International Conference on Port and Ocean Engineering under Arctic Conditions, June 9-13, Espoo, Finland. POAC13-132. 12p.

Gürtner A.,Konuk I., Gudmestad O.T. and Liferov P. 2008. Innovative Ice Protection for Shallow Water Drilling: Part III - Finite Element Modelling of Ice Rubble Accumulation. 27th International Conference on Offshore Mechanics and Arctic Engineering. OMAE2008-57915. 8p.

Hetenyi M. 1946. Beams on Elastic Foundation. The University of Michigan Press. Michigan.

Hopkins M.A. 1994. On the ridging of intact lead ice, Journal of Geophysical Research 99.

Hopkins M.A. 1998. On the four stages of pressure ridging, Journal of Geophysical Research, 103, (C10).

Izumiyama K., Irani M.B. and Timco G. W. 1994. Influence of a Rubble Field in Front of a Conical Structure. Proceedings of the Fourth International Offshore and Polar Engineering Conference, Osaka, Japan, The International Society of Offshore and Polar Engineers. pp 553-558.

Karulin E.B., Karulina M.M. and Blagovidov L.B. 2007. Ice Model Tests of Caisson Platform in Shallow Water. International Journal of Offshore and Polar Engineering, Vol 17, No4. The International Society of Offshore and Polar Engineers. pp 270-275.

Kovacs A. 1982 . Recent Shore Ice Ride-up and Pile-up Observations. Part I Beaufort Sea Coast, Alaska. Cold Regions Research & Engineering Laboratory, US Army Corps of Engineers, CRREL Report 83-9. 59p.

Kovacs A. 1983. Shore ice ride-up and pile-up features. Part II Beaufort Sea Coast – 1983 and 1984. Cold Regions Research & Engineering Laboratory, US Army Corps of Engineers, CRREL Report 84-26. 33p.

Kovacs A. and Sodhi D.S. 1980. Shore ice pile-up and ride-up: Field observations, models, theoretical analyses. Cold Regions Science and Technology 2, pp 209-288.

Leppäranta M. 2013. Land-ice interaction in the Baltic Sea. Estonian Journal of Earth Sciences, 2013, 62, 1, pp 2-14.

Li G., Braun K.W. Hudson B.K. and Sayed M. 2009. When Will Ice Ride-Up or Pile-Up Occur? Proceedings of the 20th International Conference on Port and Ocean Engineering under Arctic Conditions, June 9-12, 2009, Luleå, Sweden, POAC09-35, 10p.

Marshall A., Jordaan I. and McKenna, R. 1991. A two dimensional model of grounded ice rubble. 11th International Conference on Port and Ocean Engineering under Arctic Conditions, St. John's, Canada, POAC 91 Vol. 1, pp. 428-444.

Maattanen M. and Hoikkanen J. 1990. The Effects of Ice Pile Up on the Ice Force of a Conical Structure, Proceedings of the 10th International Symposium on Ice, Vol. 2, Espoo, Finland, pp 1010-1021.

Mayne D.C. and Brown T.G. 2000. Rubble Pile Observations. Proceedings of the Tenth International Offshore and Polar Engineering Conference, Seattle, USA, May 28-June 2, The International Society of Offshore and Polar Engineers, pp 596-599.

McKenna R., Marcellus B., Croasdale K., McGonigal D. and Stuckey P. 2008. Modelling of Ice Rubble Accumulation around Offshore Structures. Proceedings of Eighth International Conference and Exhibition on Ships and Structures in Ice, Society of Naval Architects and Marine Engineers (SNAME), Paper No. ICETECH08-116-RF, 8p.

McKenna R., Stuckey P., Fuglem M., Crocker G., McGonigal D., Croasdale K., Verlaan P. and Abuova A. 2011. Ice Encroachment in the North Caspian Sea, POAC11-002, Proceedings of the 21st International Conference on Port and Ocean Engineering under Arctic Conditions, July 10-14

Neth V. 1991. Ice rubble formation along the Molikpaq, 11th International Conference on Port and Ocean Engineering under Arctic Conditions, St. John's, Canada. pp. 241– 258.

Paavilainen J. 2013. Factors affecting ice loads during the rubbling process using a 2D FE-DE Approach. Doctoral dissertation, Aalto University School of Engineering, 58p.

Palmer A. and Croasdale K. 2012. Arctic Offshore Engineering. World Scientific Publishing, Singapore, 327p.

Ranta J., Polojarvi A. and Tuhkuri J. 2018. Limit mechanisms for ice loads on inclined structures: Buckling. Cold Regions Science and Technology. Volume 147, pp 34-44.

Saarinen S. 2000. Description of the pile up process of an ice sheet against an inclined plate. Master's thesis. Helsinki University of Technology, Department of Mechanical Engineering. 78p. (In Finnish).

Sayed M. 1989. Transmission of loads through grounded ice rubble, Proceedings of the 10th IAHR International Symposium on Ice, pp 259-275.

Sodhi D. S., Hirayama K., Haynes F. D. and Kato K. 1983. Experiments on Ice Ride-Up and Pile-Up. Annals of Glaciology 4, International Glaciological Society, pp 266-270.

Taylor R.B. 1978. The Occurrence Of Grounded Ice Ridges And Shore Ice Piling Along The Northern Coast Of Somerset Island, N.W.T. Arctic v31 No.2. pp 133-149.

Timco G. W., Sayed M. and Frederking R. M. W. 1989. Model Tests of Load Transmission Through Grounded Ice Rubble. Eighth International Conference on Offshore Mechanics and Arctic

Engineering-Vol. 1V, Editors: N. K. Sinha, D. S. Sodhi, and J. S. Chung, Book No. 10285D- 1989, The American Society of Mechanical Engineers. pp 269-274.

Timco G. 1991.The vertical pressure distribution on structures subjected to rubble forming ice. 11th International Conference on Port and Ocean Engineering under Arctic Conditions., St. John's, Canada. pp 185-197.

Timco G.W. and Wright, B.D. 1999. Load Attenuation through Grounded Ice Rubble at Tarsiut Island. Proceedings 15th International Conference on Port and Ocean Engineering under Arctic Conditions, Helsinki, Finland, POAC99 Vol. 1, pp 454-463.

Timco G.W. and Barker A. 2002. What is the Maximum Pile-Up Height for Ice? Proceedings of the 16th IAHR International Symposium on Ice, Dunedin, New Zealand, 2nd–6th December 2002. International Association of Hydraulic Engineering and Research. 141. 9p.

Tucker W.B. and Govoni J.W. 1981. Morphological investigations of first-year sea ice pressure ridge sails. Cold Regions Science and Technology, Volume 5, Issue 1, September 1981, pp 1-12.

Yoshimura N. and Inoue, M. 1985. Model tests of ice rubble field around a gravel island. Proceedings of 8th International Conference on Port and Ocean Engineering under Arctic Conditions, Narssarssuaq, Greenland, Sep. 7-14, 1985. Proceedings, Vol.2. pp 716-726.